Journal of Magnetic Resonance **148,** 221–237 (2001)
doi:10.1006/jmre.2000.2236, available online at http://www.idealibrary.com on IDEAL®

Mechanism of Relaxation Enhancement of Spin Labels in Membranes by Paramagnetic Ion Salts: Dependence on 3*d* and 4*f* Ions and on the Anions

V. A. Livshits,*,† B. G. Dzikovski,† and D. Marsh*

**Max-Planck-Institut für biophysikalische Chemie, Abteilung Spektroskopie, 37070 Göttingen, Germany; and †Centre of Photochemistry, Russian Academy of Sciences, 117427 Moscow, Russian Federation*

Received July 9, 1999; revised August 2, 2000

Progressive saturation EPR measurements and EPR linewidth determinations have been performed on spin-labeled lipids in fluid phospholipid bilayer membranes to elucidate the mechanisms of relaxation enhancement by different paramagnetic ion salts. Such paramagnetic relaxation agents are widely used for structural EPR studies in biological systems, particularly with membranes. Metal ions of the 3*d* and 4*f* series were used as their chloride, sulfate, and perchlorate salts. For a given anion, the efficiency of relaxation enhancement is in the order $Mn^{2+} \geq Cu^{2+} > Ni^{2+} > Co^{2+} \approx Dy^{3+}$. A pronounced dependence of the paramagnetic relaxation enhancement on the anion is found in the order $ClO_4^- > Cl^- > SO_4^{2-}$. This is in the order of the octanol partition coefficients multiplied by spin exchange rate constants that were determined for the different paramagnetic salts in methanol. Detailed studies coupled with theoretical estimates reveal that, for the chlorides and perchlorates of Ni^{2+} (and Co^{2+}), the relaxation enhancements are dominated by Heisenberg spin exchange interactions with paramagnetic ions dissolved in fluid membranes. The dependence on membrane composition of the relaxation enhancement by intramembrane Heisenberg exchange indicates that the diffusion of the ions within the membrane takes place via water-filled defects. For the corresponding Cu^{2+} salts, additional relaxation enhancements arise from dipolar interactions with ions within the membrane. For the case of Mn^{2+} salts, static dipolar interactions with paramagnetic ions in the aqueous phase also make a further appreciable contribution to the spin-label relaxation enhancement. On this basis, different paramagnetic agents may be chosen to optimize sensitivity to different structurally correlated interactions. These results therefore will aid further spin-label EPR studies in structural biology.

Key Words: **spin label; membrane; EPR; spin–lattice relaxation; relaxation enhancement; paramagnetic ion; Ni^{2+}; Co^{2+}; Cu^{2+}; Mn^{2+}; Dy^{3+}; $Fe(CN)_6^{3-}$; magnetic dipole–dipole interaction; Heisenberg spin exchange.**

INTRODUCTION

Motivations for the present work, which involves study of the relaxation enhancements of spin labels in membranes by various paramagnetic ion salts, are twofold. (1) Measurement of spin-label relaxation enhancements induced by interaction with paramagnetic ions, or their complexes, is a valuable and proven approach to studying the spatial distribution of spin-labeled functional groups of both phospholipids and proteins in membranes (*1–5*). However, to obtain reliable structural information from such spin-label EPR measurements, the mechanisms of the enhancements need to be clearly understood in the various cases. Both distance-dependent dipolar interactions (*3, 6*) and Heisenberg exchange interactions (*5*) have been used in such studies, depending on the chemical nature of the paramagnetic relaxant. (2) There are many studies on permeability and diffusion of small nonelectrolyte molecules (including oxygen) in lipid membranes (*7–9*), as well as on the permeability of univalent ions (*10, 11*). Divalent cations (other than Ca^{2+} and Mg^{2+} of the normal physiological milieu) are known to affect the activity of a number of cytoplasmic and membrane proteins. However, only limited data are available on the permeability or transbilayer and lateral diffusion of these ions in lipid membranes (*7, 12, 13*). Such information can be provided by spin exchange contributions to the relaxation enhancements if they are controlled by the collisional dynamics between spin label and relaxant [e.g. (*14, 15*)].

In the present paper, spin-labeled phospholipids with different positions of the nitroxide moiety in the acyl chain are used in lipid bilayer membranes. This is done both to elucidate the mechanisms and efficiency of spin-label relaxation enhancements by different paramagnetic metal ions and to obtain information on the partitioning and diffusion of divalent ions in membranes. The relaxation enhancements by paramagnetic ions from the 3*d* (Cu^{2+}, Ni^{2+}, Co^{2+}, Mn^{2+}, Fe^{3+}) and 4*f* (Dy^{3+}) series, which differ considerably in both their spin–lattice relaxation times and their electron spin values, are compared. Further, the role of the anionic counter ions, and also that of the lipid phase state and composition of the membrane, in determining the relaxation enhancements is studied.

Progressive saturation techniques with integrated EPR intensities and amplitudes are used for measuring the spin relaxation parameters. The advantage of using the second integrals,

1090-7807/01 $35.00

rather than spectral amplitudes, is that these do not depend on the degree of inhomogeneous broadening in the EPR spectra (*16*). In a previous paper (*17*), a method was developed for determining the relaxation parameters from microwave-power saturation curves that took account of both the Zeeman field modulation and isotropic molecular motion of the spin labels. For the present work, this method is extended to include anisotropy of the molecular motion, as is necessary for spin-labeled lipids in fluid membranes.

It is found that partitioning of the paramagnetic ions into the membrane (most probably as ion pairs) can be of considerable importance, and—depending on the anion—may be of overwhelming importance. In consequence, direct Heisenberg spin exchange interactions, rather than distance-dependent static magnetic dipolar interactions with ions in the aqueous phase, can come to dominate the relaxation enhancements. This is especially the case for membranes in the biologically relevant fluid phase and for particular anionic counterions such as perchlorate. For these cases (i.e., spin exchange interactions), the relaxation enhancements provide additional information that relates to the partitioning and dynamics of the paramagnetic ions within the membrane.

MATERIALS AND METHODS

Spin-labeled phosphatidylcholines, *n*-PCSL (1-acyl-2-[*n*-(4,4-dimethyloxazolidine-*N*-oxyl)stearoyl]-*sn*-glycero-3-phosphocholine) with $n = 5$, 8, 10, 14, or 16, were synthesised according to Ref. (*18*). Synthetic phosphatidylcholine, DMPC (1,2-dimyristoyl-*sn*-glycero-3-phosphocholine), was from Avanti Polar Lipids (Alabaster, AL) and egg yolk phosphatidylcholine (PC) was from Fluka (Buchs, Switzerland). Cholesterol was from Merck (Darmstadt). The paramagnetic salts $NiCl_2$, $CuCl_2$, $CoCl_2$, $MnCl_2$, $DyCl_3$, $Ni(ClO_4)_2$, $Cu(ClO_4)_2$, $NiSO_4$, $MnSO_4$, and $K_3(FeCN)_6$ were from Sigma (St. Louis, MO) and Fluka; methanol and *n*-octanol were of analytical grade.

Spin-labeled phosphatidylcholines were incorporated in bilayer membranes of DMPC or egg PC at a relative concentration of 1 mol% by drying down the lipid solutions in chloroform and then suspending the dry lipid in water. The concentration of paramagnetic salts in the aqueous phase of the lipid dispersions was either 10 or 30 mM. All membrane dispersions (and also methanol solutions) were saturated with argon. Aliquots of the samples were loaded into 50-μl, 0.7-mm-id glass capillaries (Brand, Germany) and flushed with argon. Sample sizes were trimmed to 5-mm length to avoid inhomogeneities in the H_1 and H_m fields (*19*).

Partition coefficients of the paramagnetic salts in octanol/water were determined as follows. *N*-Octanol was added to a 1 M aqueous solution of the salt in a volume ratio of 2.5 ml/l ml. The mixture was vigorously shaken for 2 h, left to equilibrate for 10 min, and centrifuged for 15 min at 13000 rpm. The upper part of the octanol fraction was removed and centrifuged again. A total of 1.6 ml of the resulting octanol fraction was mixed with 1.6 ml of water for back-extraction, and the procedure was repeated. The aqueous fraction was taken and used for metal ion determination. The metal ion concentrations were measured on an atomic absorption spectrometer with an accuracy of 0.005 ppm. The solutions were diluted 10-fold before the measurements. In the case of copper and nickel perchlorates and chlorides, the metal ion concentrations were also determined colorimetrically using metal indicators dimethylglyoxime and dithizone for Ni^{2+} and Cu^{2+} ions, respectively.

EPR spectra were recorded at a microwave frequency of 9 GHz on a Varian Century Line or Bruker EMX spectrometer equipped with nitrogen gas flow temperature regulation. Sample capillaries were positioned along the symmetry axis of the standard 4-mm quartz EPR sample tube that contained light silicone oil for thermal stability. Temperature was measured with a fine-wire thermocouple located within the capillary in contact with the sample. Samples were centered in the TE_{102} rectangular microwave cavity and all spectra were recorded under critical coupling conditions. The root-mean-square microwave magnetic field $\langle H_1^2 \rangle^{1/2}$ at the sample was measured as described in Ref. (*19*), and corrections were made for the cavity Q as described in the same reference. The in-phase EPR spectra were recorded in the first-harmonic absorption mode at a modulation frequency of 100 kHz. The modulation field measured at the sample was 0.32 G p-p.

Water proton NMR linewidths from the residual HDO in D_2O were measured at 25°C for aqueous solutions of the various Ni^{2+} and Cu^{2+} salts at 30 mM and the Mn^{2+} salts at 10 mM on a Bruker DRX-500 spectrometer. Corresponding EPR linewidths were measured for the Cu^{2+} and Mn^{2+} salts at the same temperature on a Bruker ER-200 9-GHz spectrometer. The dependence on anion was small in each case, indicating that differences in spin-label relaxation enhancements that are reported here cannot be attributed to a dependence on the anion of the relaxation parameters of the paramagnetic ions in the aqueous phase.

THEORETICAL BACKGROUND

Progressive Saturation and Spin–Lattice Relaxation Enhancements

In CW progressive saturation experiments, one determines a saturation parameter, P, by fitting saturation curves for the double integral, I, of the EPR spectrum to the equation

$$I = \frac{I_o \cdot H_1}{(1 + P \cdot H_1^2)^{1/2}}, \qquad [1]$$

where $P = \gamma_e^2 \cdot T_1 T_2^{eff}$, and T_2^{eff} is an effective spin–spin relaxation time that takes into account the relaxation contribution from rotational motion of the spin label (*14*). In the

presence of a paramagnetic relaxation agent at concentration c_R, the spin–lattice relaxation rate, T_1^{-1}, is given by

$$T_1^{-1} = T_{1,o}^{-1} + k_{RL}c_R, \qquad [2]$$

where $T_{1,o}$ is the intrinsic spin–lattice relaxation time and k_{RL} is a constant that depends on the collision rate in the case of Heisenberg spin exchange or on the distance of closest approach in the case of a static dipole–dipole interaction with the paramagnetic relaxant. If the contribution of paramagnetic enhancement to $(T_2^{eff})^{-1}$ is equal to that for T_1^{-1}, then the resulting change in saturation parameter, P, of the spin label is given by

$$\Delta(1/P) = (\gamma_e^2 T_{2,o}^{eff})^{-1} k_{RL}c_R, \qquad [3]$$

where it is assumed that $k_{RL}c_R \ll (T_{2,o}^{eff})^{-1}$, and $T_{1,o} \gg T_2^{eff}$. Typically, $T_{1,o}$ (≈ 1 μs) is an order of magnitude, or more, greater than T_2^{eff}, which has values ≈ 3–7×10^{-8} s from linewidth measurements.

Static Dipolar Enhancements of T_1 Relaxation

The relaxation enhancement contributed by a static magnetic dipole–dipole interaction between the spin label and a paramagnetic ion arises from modulation of the dipolar interaction by the rapid spin–lattice relaxation of the latter. The enhancement by a single paramagnetic ion, i, may be derived from the Solomon–Bloembergen equation for electron spins [see, e.g., (*20, 21*)] as

$$\frac{1}{T_{1,dd}^{(i)}\,(\text{static})} = \frac{|\boldsymbol{\mu}_R|^2\gamma_e^2}{6r_i^6}\left\{(1 - 3\cos^2\Omega_i)^2 \times \frac{T_{2,R}}{1 + (\omega_L - \omega_R)^2 T_{2,R}^2} + \frac{9}{2}\sin^2 2\Omega_i \frac{T_{1,R}}{1 + \omega_L^2 T_{1,R}^2} + 9\sin^4\Omega_i \frac{T_{2,R}}{1 + (\omega_L + \omega_R)^2 T_{2,R}^2}\right\}, \qquad [4]$$

where ω_R and ω_L are the Larmor frequencies of the paramagnetic ion and spin label, respectively, r_i is the separation of the spin label and paramagnetic ion, Ω_i is the angle between the interdipole vector $\mathbf{r}_i$ and the magnetic field direction, $T_{1,R}$ and $T_{2,R}$ ($=T_{1,R}$) are the spin–lattice and spin–spin relaxation times, respectively, of the paramagnetic ion, and $\boldsymbol{\mu}_R$ ($=g_R\beta_e\mathbf{S}_R$) is its magnetic moment operator. In terms of polar coordinates defined relative to the membrane normal, the angle Ω_i is given by

$$\cos\Omega_i = \cos\theta_i\cos\theta_0 + \sin\theta_i\sin\theta_0\cos\varphi_i, \qquad [5]$$

where θ_0 and θ_i are, respectively, the angles that the magnetic field and interspin vector $\mathbf{r}_i$ make with the membrane normal, and φ_i is the azimuthal orientation of $\mathbf{r}_i$ relative to the magnetic field direction.

Paramagnetic ions, i, distributed in the aqueous phase or adsorbed at the lipid–water interface give additive contributions to $T_{1,dd}^{-1}$ (static). Volume integration, in the first case, and surface integration, in the second case, over the polar coordinates r_i, θ_i, and φ_i of the paramagnetic ions give values of $T_{1,dd}^{-1}$ (static) that are dependent on the magnetic field orientation θ_0. For volume integration over the paramagnetic ion distribution, the required terms in Eq. [4] are

$$\int \frac{(1 - 3\cos^2\Omega)^2}{r^6}\,dV = \frac{\pi}{4R^3}\left(\cos^2\theta_0 + \frac{3}{8}\sin^4\theta_0\right)$$

$$\int \frac{\sin^2 2\Omega}{r^6}\,dV = \frac{\pi}{9R^3}\left(1 - \frac{3}{8}\sin^4\theta_0\right)$$

$$\int \frac{\sin^4\Omega}{r^6}\,dV = \frac{\pi}{36R^3}\left(4 - 3\cos^2\theta_0 + \frac{3}{8}\sin^4\theta_0\right), \qquad [6]$$

where R is the distance of closest approach of ions to the spin label, which is directed along the membrane normal. Analogous expressions are obtained in the case of surface distributions of paramagnetic ions.

In saturation experiments with macroscopically unoriented suspensions, one measures saturation parameters for the membranes that are randomly oriented with respect to the static magnetic field direction, i.e., for spin packets with different values of θ_0 ($0 \le \theta_0 \le \pi/2$). However, it can be seen from Eq. [6] that the residual angle dependence of $T_{1,dd}^{-1}$ (static) on θ_0 is much weaker than its initial dependence on Ω that is given in Eq. [4]. Therefore, for reasonable estimates, one can average $T_{1,dd}^{-1}$ (static) over θ_0 and use angular independent expressions for $T_{1,dd}^{-1}$ (static). For volume and surface distributions, respectively, one obtains

$$T_{1,dd}^{-1}\,(\text{static}) = \frac{\pi}{45}\frac{\mu_R^2\gamma_e^2}{R^3}\,T_{1,R}\cdot c\cdot f_1(\omega_L, \omega_R) \qquad [7]$$

$$T_{1,dd}^{-1}\,(\text{static}) = \frac{\pi}{15}\frac{\mu_R^2\gamma_e^2}{R^4}\,T_{1,R}\cdot c_s\cdot f_1(\omega_L, \omega_R), \qquad [8]$$

with

$$f_1(\omega_L, \omega_R) = \frac{1}{1 + (\omega_L - \omega_R)^2 T_{1,R}^2} + \frac{3}{1 + \omega_L^2 T_{1,R}^2} + \frac{6}{1 + (\omega_L + \omega_R)^2 T_{1,R}^2}, \qquad [9]$$

TABLE 1

Numerical Estimates of Enhancements in T_1- and T_2-Relaxation Rates of Spin Labels in Membranes by Static Dipolar Interactions with 30 mM Aqueous Paramagnetic Ions, and $R = 1$ nm in Eqs. [7]–[9] and Eqs. [10]–[12] for $T_{1,dd}^{-1}$ and $T_{2,dd}^{-1}$, Respectively

				$T_{1,dd}^{-1}$ (s^{-1})		$T_{2,dd}^{-1}$ (s^{-1})	
Ion, R	$\langle g_R \rangle$	S_R	$T_{1,R}(s)$[b]	Volume	Surface[a]	Volume	Surface[a]
Ni^{2+}	2.25	1	3×10^{-12}[b]	0.8×10^{4}[c]	3.9×10^{4}	0.9×10^{4}	4.3×10^{4}
			5×10^{-12}[d]	1.1×10^{4}[c]	5.4×10^{4}	1.3×10^{4}	6.6×10^{4}
Co^{2+}	4.33	1/2	$\approx 10^{-12}$[e]	4.6×10^{3}	2.2×10^{4}	4.6×10^{3}	2.2×10^{4}
Cu^{2+}	2.2	1/2	1×10^{-9}[f]	4×10^{3}	2.5×10^{4}	2.4×10^{5}	1.5×10^{6}
			3×10^{-9}[f]	1.4×10^{3}	0.9×10^{4}	7.3×10^{5}	4.6×10^{6}
Mn^{2+}	1.993	5/2	1×10^{-9}[g]	1×10^{6}[h]	1.1×10^{7}	2.8×10^{6}	3.1×10^{7}
			3.5×10^{-9}[i]	1.5×10^{6}[h]	1.6×10^{7}	8.9×10^{6}	9.6×10^{7}
Dy^{3+}	1.33	15/2	3.5×10^{-13}[j]	1.3×10^{4}[h]	1.9×10^{5}	1.3×10^{4}	1.9×10^{5}
			8×10^{-13}[f]	3.0×10^{4}[h]	4.5×10^{5}	3.0×10^{4}	4.5×10^{5}

[a] Surface concentrations of Ni^{2+}, Co^{2+}, Cu^{2+}, and Mn^{2+} ions were calculated from the intrinsic binding constants given in (*28*): Ni^{2+} (2.9×10^{12} cm^{-2}), Co^{2+} (2.9×10^{12} cm^{-2}), Mn^{2+} (6.5×10^{12} cm^{-2}), and in our unpublished electrophoresis data Cu^{2+} (3.8×10^{12} cm^{-2}). There are no data available on binding of Dy^{3+} ions to membranes. One expects, however, that its binding constant is greater than for divalent ions, so a maximum value of $c_s = 9 \times 10^{12}$ cm^{-2} was used in this case.

[b] Reference (*22*) accounting for dynamic zero-field splitting in determining $T_{1,R}$.

[c] Accounting for zero-field splitting in determining spin-label relaxation enhancements.

[d] Reference (*23*) accounting for static zero-field splitting in determining $T_{1,R}$.

[e] Reference (*24*).

[f] Reference (*25*).

[g] Reference (*30*).

[h] Without accounting for zero-field splitting in determining spin-label relaxation enhancements (see text).

[i] Reference (*25*) accounting for static zero-field splitting in determining $T_{1,R}$.

[j] Reference (*26*).

where c and c_s are the bulk and surface ion concentrations, in ions/cm^3 and ions/cm^2, respectively, and $\mu_R^2 = g_R^2 \beta_e^2 S_R(S_R + 1)$, with β_e as the Bohr magneton.

Estimates of Static Dipolar T_1 Enhancements

Estimates of the static magnetic dipolar relaxation enhancement, $T_{1,dd}^{-1}$ (static), for various paramagnetic ions of interest, Ni^{2+}, Cu^{2+}, Co^{2+}, Mn^{2+}, and Dy^{3+}, can be made from Eqs. [7]–[9] by using the values of $T_{1,R}$ and g_R-factors that are known from NMR relaxation and EPR measurements for the aqua complexes of these ions (*22–27*). These estimates were made for $R = 1$ nm and a bulk paramagnetic ion concentration of 30 mM. In the case of ion adsorption at the lipid–water interface, the ion binding constants measured by electrophoresis (*28*) were used to determine the values of the surface concentration c_s corresponding to a bulk concentration of 30 mM.

For ions with $S > \frac{1}{2}$, it is necessary to take into account zero-field splittings. This can affect both the determination of $T_{1,R}$ from solvent NMR T_1-relaxation dispersion and the spectral densities (Eq. [9]) used to calculate the spin-label relaxation enhancement (see footnotes to Table 1). The latter were calculated in a manner similar to that used previously for NMR relaxation enhancements (*23, 25*). For Ni^{2+}, a value of $D = 2.5$ cm^{-1} was used for the zero-field splitting and the spin-label relaxation enhancements were averaged over the angle between the principal axis of the Ni^{2+}–aquo complex and the interspin vector (*23*). Qualitatively, the result is to reduce the spin-label relaxation enhancement because of the increased effective values of ω_R in Eq. [9]. For high-spin Co^{2+} in octahedral or tetragonally distorted hexa–aquo complexes, the combined effect of the large crystal-field splitting and spin–orbit coupling yields an isolated Kramers doublet as ground state. In this case (cf. Table 1), the net effect is to reduce the total spin of Co^{2+} to an effective value of $S_R = \frac{1}{2}$ with a g-value of 4.33 and no zero-field splitting (see, e.g., *29*). For Mn^{2+}, the zero-field splitting of aquo complexes is small, and its effect on NMR relaxation dispersion was found to be insignificant at magnetic fields corresponding to 9-GHz EPR (*27*). Therefore zero-field splitting was neglected in calculating the spin-label relaxation enhancements, which means that these are upper estimates for Mn^{2+}.

For both Ni^{2+} and Co^{2+}, $\omega^2 T_{1,R}^2 \ll 1$ and all three terms in the spectral density contribute, whereas for Cu^{2+} and Mn^{2+}, $\omega^2 T_{1,R}^2 \gg 1$ and the first term in $f_1(\omega_L, \omega_R)$ dominates at 9 GHz. The various EPR parameters of the different aqueous paramagnetic ions and the T_1-relaxation enhancements predicted under the experimental conditions stated above are given in Table 1. The values of $T_{1,dd}^{-1}$ (static) are predicted to be rather small for the first three ions in Table 1, in the order $Ni^{2+} > Co^{2+} \approx Cu^{2+}$,

but they are expected to be much greater for Mn^{2+} because of the favorable values of $T_{1,R}$ and spin S_R. For Dy^{3+}, the magnetic moment is very large because of the lack of orbital quenching for $4f$ ions, and values of the Landé g-factor $g_J = 1.33$ and total angular momentum $J = 15/2$ were used to estimate the dipolar relaxation enhancements. Nevertheless, the predicted values of $T_{1,dd}^{-1}$ are still relatively small because of the very short spin–lattice relaxation time that is characteristic of lanthanide ions (other than Gd^{3+}) at ambient temperatures. A similar situation (i.e., $\omega T_{1,R} \ll 1$) probably obtains with $Fe(CN)_6^{3-}$, for which $T_{1,R} = 2.3 \times 10^{-11}$ s at 77 K (*20*). However, values of $T_{1,R}$ have not been determined for this ion at ambient temperatures and therefore it is excluded from Table 1.

One should note that the above estimates are approximate in some respects. The effects of hyperfine structure on the resonance frequencies, ω_R, in the case of Cu^{2+} and Mn^{2+} ions, are neglected in Eq. [9]. Also, the values of $T_{1,R}$ for adsorbed ions may differ substantially from those of the aqua complexes. Furthermore, irrespective of the absolute magnitudes, it is clear from the above estimates that the values of $T_{1,dd}^{-1}$ (static) can increase by up to almost an order of magnitude for strongly adsorbed cations, because of the decreased average spin label–ion separation.

Static Dipolar Enhancements of T_2 Relaxation

The contribution, $T_{2,dd}^{-1}$ (static), to the spin–spin relaxation rate that arises from static dipolar interactions of a spin label with paramagnetic ions modulated by spin–lattice relaxation of the latter must also be considered, in relation to both progressive saturation and linewidth measurements (*20*, *30*). According to Leigh theory, the dipolar interaction between a spin label and a fast-relaxing paramagnetic ion leads mostly to a decrease in EPR amplitude rather than to line broadening, because the strong angle dependence of the static dipolar relaxation results in drastic broadening, except for interspin vectors oriented close to the magic angle (*30*). However, as in the situation for $T_{1,dd}^{-1}$ (static) just treated, this angle dependence is substantially decreased after integration over the volume or surface ion distribution (see Eq. [6]). This then results in a line broadening, rather than the apparent amplitude quenching that is obtained for two isolated dipoles in Leigh theory. The angular-independent expressions for $T_{2,dd}^{-1}$ (static) that are obtained in a similar way to those for $T_{1,dd}^{-1}$ (static) are

$$T_{2,dd}^{-1}\,(\text{static}) = \frac{\pi \cdot \mu_R^2 \cdot \gamma_e^2}{90R^3}\, T_{1,R} \cdot c \cdot f_2(\omega_L, \omega_R) \qquad [10]$$

$$T_{2,dd}^{-1}\,(\text{static}) = \frac{\pi \cdot \mu_R^2 \cdot \gamma_e^2}{30R^4}\, T_{1,R} \cdot c_s \cdot f_2(\omega_L, \omega_R), \qquad [11]$$

where

$$f_2(\omega_L, \omega_R) = 4 + \frac{1}{1 + (\omega_L - \omega_R)^2 T_{1,R}^2} + \frac{3}{1 + \omega_L^2 T_{1,R}^2} + \frac{6}{1 + \omega_R^2 T_{1,R}^2} + \frac{6}{1 + (\omega_L + \omega_R)^2 T_{1,R}^2}. \qquad [12]$$

We note that for Cu^{2+} and Mn^{2+} ($T_{1,R} \approx 10^{-9}$ s) the first term in $f_2(\omega_L, \omega_R)$ dominates, which results in $f_2(\omega_L, \omega_R) \approx 4$. On the other hand, for Ni^{2+}, Co^{2+}, and Dy^{3+}, all terms in the spectral density contribute and $f_2(\omega_L, \omega_R) \approx 20$.

Using the same values of $R = 1$ nm and a bulk ion concentration of 30 mM as for the estimations of $T_{1,dd}^{-1}$ (static), one obtains the values of T_2-relaxation enhancement that are given in Table 1. The angular-independent values of $T_{2,dd}^{-1}$ (static) estimated for Ni^{2+} ions are about 50 times smaller than for Cu^{2+} ions, both for volume and surface ion distributions. In turn, the values of $T_{2,dd}^{-1}$ (static) for Mn^{2+} ions are about 10–20 times greater than for Cu^{2+} ions.

Relaxation by Spin Exchange Interactions

Relaxation is mediated by Heisenberg spin exchange only if the paramagnetic ions come into direct contact with the spin label. For strong exchange, the rate of Heisenberg exchange is determined by the collision rate constant k_{RL} of Eq. [2] that can be obtained from the Smoluchowski equation [see also (*5*)]:

$$k_{RL} = 4\pi\sigma_{RL} r_{RL} D_T(z), \qquad [13]$$

where $D_T(z)$ is the local (isotropic) translational diffusion coefficient of the ion pair (assumed greater than for the lipids), r_{RL} is the interaction distance between ion and spin label, and σ_{RL} is a steric factor ($\approx$1). The relaxation enhancement from Heisenberg exchange, $T_{1,HE}^{-1} = k_{RL} n_R$, is then obtained by the combination of Eqs. [2] and [13]. In Eq. [13], however, it is assumed that the local ion concentration $n_R(z)$ at distance z along the membrane normal, which appears in Eqs. [2] and [3], is expressed in ions per unit volume, rather than in molar units which was designated by c_R. It should be noted that Heisenberg exchange contributions to the T_2 relaxation rate are equal to those for T_1 relaxation, i.e., $T_{2,HE}^{-1} = T_{1,HE}^{-1}$ (*31*).

Dynamic Dipolar Relaxation Enhancements

In the case of rapid translational diffusion, spin-label relaxation can be induced by the modulation of the dipolar interactions that arises from the mutual diffusive motions of the spin labels and paramagnetic ions. Unlike the situation for Heisenberg exchange, the contribution of dynamic dipolar interactions to T_2 relaxation is greater than the contribution to T_1 relaxation. This arises from the contributions to T_2 relaxation of spectral densities at low frequencies. Dynamic dipolar relaxation is characterized by the dipolar correlation time $\tau_D =$

$r_{RL}^2/2D_T$, and the criterion that the dynamic mechanism dominates over the static relaxation mechanism is $\tau_D^{-1} \gg T_{1,R}^{-1}$ and vice versa (see, e.g., Ref. *32*). For the case that dynamic dipolar relaxation dominates, the T_2 enhancement is given by (*32*)

$$T_{2,dd}^{-1}\,(\text{dynamic}) = \mu_R^2\gamma_e^2\left[\frac{1}{6}\,J^{(0)}(0) + \frac{1}{24}\,J^{(0)}(\omega_R - \omega_L)\right], \qquad [14]$$

where ω_R and ω_L are the electron Larmor frequencies of the paramagnetic ion and spin label, respectively. In Eq. [14], spectral densities, $J^{(k)}(\omega)$, at the Larmor frequency and above are assumed to be negligible compared with those at low frequency (*33*) and therefore are omitted. For ions (e.g., Mn^{2+}) with g-values close to the spin label g-value, such that $(\omega_R - \omega_L)^2\tau_D^2 \ll 1$, it can be assumed that $J^{(0)}(\omega_R - \omega_L) \approx J^{(0)}(0)$. For ions with $(\omega_R - \omega_L)^2\tau_D^2 \gg 1$, on the other hand, the relaxation term involving $J^{(0)}(\omega_R - \omega_L)$ may be neglected. With the zero-frequency spectral density for translational diffusion given by $J^{(0)}(0) = (48\pi/15^2)n_R/(D_T r_{RL})$ (*32*), the T_2-relaxation enhancement becomes

$$T_{2,dd}^{-1}\,(\text{dynamic}) = C\cdot\mu_R^2\gamma_e^2 n_R/(D_T r_{RL}), \qquad [15]$$

where $C = 2\pi/45$ for $(\omega_R - \omega_L)^2\tau_D^2 \ll 1$, and $C = 8\pi/15^2$ for $(\omega_R - \omega_L)^2\tau_D^2 \gg 1$.

In contrast, the corresponding expression for the dynamic dipolar enhancement in T_1 relaxation is (*32*)

$$T_{1,dd}^{-1}\,(\text{dynamic}) = \frac{1}{12}\,\mu_R^2\gamma_e^2 J^{(0)}(\omega_R - \omega_L), \qquad [16]$$

i.e., $T_{1,dd}^{-1} = (2/5)T_{2,dd}^{-1}$ for $(\omega_R - \omega_L)^2\tau_D^2 \ll 1$, and $T_{1,dd}^{-1} \ll T_{2,dd}^{-1}$ for $(\omega_R - \omega_L)^2\tau_D^2 \gg 1$. Therefore, for ions with g-values that differ considerably from that of the spin label ($\Delta g \gg 0.01$), the dynamic dipolar T_1 relaxation is expected to be small. For ions with g-values close to those of the spin label ($\Delta g < 0.01$), the T_1-relaxation enhancement is two-fifths that of the dynamic dipolar T_2 relaxation rate.

RESULTS

Paramagnetic relaxation enhancements were determined for phospholipids spin-labeled in the *sn*-2 chain by using progressive saturation methods. Most of the measurements are confined to fluid lipid bilayers in the L_α-phase, which corresponds to the dynamic state of biological membranes at physiological temperatures, and concentrate on the nature of the paramagnetic relaxant. Results on the intermediate $P_{\beta'}$ gel phase are presented later. A range of paramagnetic ions is used which differ in their electron spin, g-values, and T_1 relaxation times, in order to discriminate between the dipolar and exchange relaxation enhancement mechanisms. Different anions are also used because these may affect ion solubility in the membrane. Ni^{2+} ions are favored for further experiments on temperature dependence and membrane composition because Ni^{2+} gives reasonably large relaxation enhancements and no background EPR signal and has been used extensively in previous membrane studies.

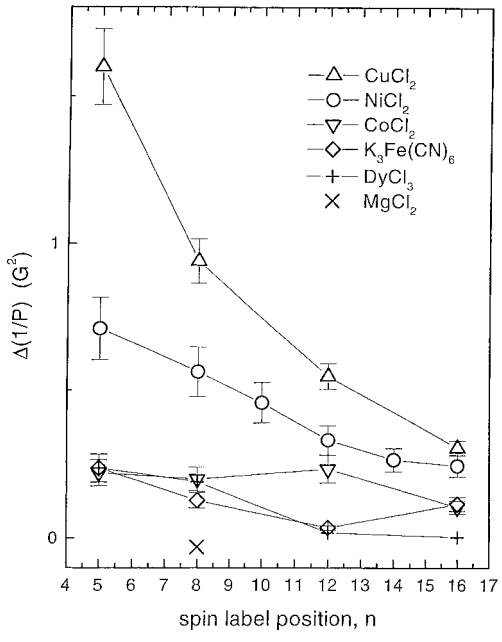

FIG. 1. Dependence of the $\Delta(1/P)$ relaxation enhancement parameter on labeling position, n, of n-PCSL spin labels in DMPC membranes at 39°C. Data are given for different paramagnetic ion chlorides at a bulk concentration of 30 mM: $CuCl_2$ (△), $NiCl_2$ (○), $CoCl_2$ (▽), $DyCl_3$ (+), and for $K_3Fe(CN)_6$ (◇). The cross (×) indicates the value of $\Delta(1/P)$ for the diamagnetic control, 30 mM $MgCl_2$.

Dependence on Paramagnetic Ion

The dependence of the relaxation enhancement parameter, $\Delta(1/P)$, on spin label position, n, of n-PCSL probes in fluid-phase DMPC membranes is given for the interaction with different paramagnetic ion chlorides in Fig. 1. An equivalent concentration of $MgCl_2$ was used as a nonparamagnetic control. The value of $\Delta(1/P)$ for 8-PCSL was zero in the presence of 30 mM $MgCl_2$, which shows that the enhancements observed are entirely due to paramagnetic contributions. It is seen that the paramagnetic relaxation enhancement is greatest for Cu^{2+} and decreases in the order $Cu^{2+} > Ni^{2+} > Co^{2+} \approx Fe(CN)_6^{3-} \approx Dy^{3+}$. This progression is not entirely in accord with the estimates of the static dipolar contributions to the relaxation enhancements that were given in the previous section (cf. Table 1). The larger values of $\Delta(1/P)$ for Cu^{2+} and Ni^{2+} chlorides, compared to those of Co^{2+} and Dy^{3+}, do not correlate with the corresponding estimates of $T_{1,dd}^{-1}$ (static) and $T_{2,dd}^{-1}$ (static). Also, the relaxation enhancement does not decrease monotonically with increasing values of n, for all ions.

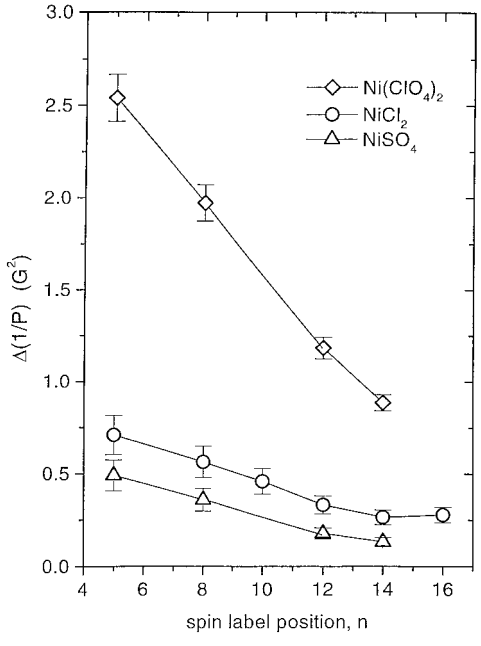

FIG. 2. Dependence of the $\Delta(1/P)$ relaxation enhancement parameter on spin-label position, n, for 30 mM bulk concentration of Ni^{2+} salts with different anions: $Ni(ClO_4)_2$ (◇), $NiCl_2$ (○), and $NiSO_4$ (△). Data are given for n-PCSL spin labels in DMPC membranes at 39°C.

For those ions for which it does, fits to the $1/R^3$ or $1/R^4$ dependence on separation predicted for a static magnetic dipole–dipole relaxation do not yield entirely consistent values of the fitting parameters.

In principle, the relaxation data could be consistent, however, with a mechanism for the enhancement that is due to Heisenberg spin exchange or dipole–dipole interaction between spin labels and paramagnetic ions which may partition into the membrane.

Dependence on Anion

In order to distinguish further between the different mechanisms, the dependence of the relaxation enhancement on the nature of the counterion was studied. The dependences on spin-label position, n, of the $\Delta(1/P)$ enhancement parameter for Ni^{2+} ions with ClO_4^-, Cl^-, and SO_4^{2-} anions and fluid DMPC membranes are given in Fig. 2. The values of $\Delta(1/P)$ are considerably greater for $Ni(ClO_4)_2$ than for $NiCl_2$, for all values of n; the dependence on n is also steeper and is approximately linear. In turn, the values of $\Delta(1/P)$ for $NiCl_2$ are somewhat greater than those for $NiSO_4$. A similar relative order was found also for Mn^{2+} chloride and sulfate, with fluid DMPC membranes (see later).

The value of $\Delta(1/P)$ for 5-PCSL in the presence of 30 mM $Mg(ClO_4)_2$ was also measured as a diamagnetic control and found to be small and equal to -0.07 G^2, indicating that the strong positive effect of Ni^{2+} (and Cu^{2+}) perchlorate is due entirely to the paramagnetic properties of these ions. The slightly negative value of $\Delta(1/P)$ for $Mg(ClO_4)_2$ is probably attributable to a decrease in rotational mobility (and hence increase in T_2^{eff}) of the spin labels that is seen in the corresponding linear EPR spectra (see later).

Most Ni^{2+}, Cu^{2+}, and Mn^{2+} salts are strong electrolytes. At 30 mM concentration in water the chlorides and perchlorates almost fully dissociate, i.e., the cations exist in water as the aqua complexes. The degrees of dissociation, estimated from critical stability constants, are 0.98, 0.97, 0.99, and 0.97 for 30 mM $NiCl_2$, $CuCl_2$, $MnCl_2$, and $CoCl_2$, respectively. Those for the perchlorate salts are expected to be even greater. Only for the sulfates are they considerably smaller (approximately 0.5 for 30 mM $NiSO_4$ and $MnSO_4$). Further, experiments have been performed that demonstrate that there is little effect of anions on the relaxation properties of the various aqueous paramagnetic ions, either from ion pairing or from any other aqueous mechanism. Both the water proton NMR linewidths and the paramagnetic ion EPR linewidths (for Cu^{2+} and Mn^{2+}) show only small variations with anion for the aqueous paramagnetic salts. Manganese salts show the most appreciable dependence on anion and that is only an approximately 10% variation. Therefore, the pronounced effects of anions on the spin-label relaxation enhancements cannot arise from a mechanism involving paramagnetic ions in the aqueous phase. Also, the dependences on anionic counterions that are almost fully dissociated in water cannot be explained in terms of a dipole–dipole interaction of spin labels with paramagnetic ion–anion complexes located in the aqueous phase or adsorbed at the lipid–water interface. On the other hand, they can be due to partitioning of the paramagnetic ions into the lipid membrane most probably as cation–anion pairs. Then direct Heisenberg spin exchange, or either a static or a collision-controlled dipolar interaction, with the spin labels could account for the relaxation enhancement. In particular, perchlorates of univalent or divalent ions are known to be partly soluble in polar organic solvents (e.g., acetonitrile, acetone, or dimethyl formamide) (*34, 35*). Partitioning of divalent cations into the membrane is expected to take place as compensating ion pairs on electrostatic grounds, because of the high Born energy penalty of burying a highly charged ion of small radius in a medium of low dielectric constant (see, e.g., Ref. *12*).

Paramagnetic Salts in Organic Solvent

To obtain additional information relevant to the ion partitioning hypothesis, the n-octanol/water partition coefficients (K_p) of the different salts were measured by using atomic absorption spectroscopy (Table 2). Some of the larger values were confirmed by colorimetric measurements using indicator dyes. The dependence of the partition coefficient on the anion (for a given paramagnetic cation) is very clear in Table 2. Partitioning into the more hydrophobic environment is in the order perchlorate > chloride > sulfate.

In addition, the Lorentzian line broadening in the EPR

TABLE 2

Properties of Paramagnetic Salts in Nonaqueous Solvents: Partition Coefficient, K_p, between *n*-Octanol and Water and Biomolecular Rate Constant, k_{ex}, for Spin Exchange with the 10-PCSL Spin Label in Methanol

Paramagnetic salt	K_p	$k_{ex} \times 10^{-9}$ (s^{-1} M^{-1})[a]	$K_p \cdot k_{ex}$ (s^{-1} M^{-1})
$Ni(ClO_4)_2$	12.2×10^{-3}	1.3 ± 0.1	1.6×10^7
$NiCl_2$	4.46×10^{-4}	1.1 ± 0.1	4.9×10^5
$NiSO_4$	1.53×10^{-6}	0.67 ± 0.1	1.0×10^3
$Cu(ClO_4)_2$	14.2×10^{-3}	1.9 ± 0.1	2.7×10^7
$CuCl_2$	1.75×10^{-3}	1.8 ± 0.1	3.1×10^6
$CoCl_2$	4.69×10^{-4}	0.13 ± 0.02	6.1×10^4
$DyCl_3$	8.4×10^{-5}	~ 0.05	$\sim 4 \times 10^3$
$MnCl_2$	5.02×10^{-4}	1.6 ± 0.1	8.0×10^5
$MnSO_4$	2.04×10^{-6}	0.77 ± 0.2[b]	1.6×10^3
$K_3Fe(CN)_6$	$<10^{-6}$	0.072 ± 0.02[b]	$<10^2$

[a] Measured from the peak-to-peak linewidth, $\Delta H^{pp} + 0.783$ G, where the correction is for inhomogeneous broadening (*36*).

[b] Measured in 50% v/v methanol/H_2O mixture.

spectrum of the 10-PCSL spin label by paramagnetic ions was measured in methanol. Corresponding bimolecular exchange rate constants (k_{ex}) were calculated by assuming that the paramagnetic broadening was attributable solely to collisional spin exchange in this low-viscosity solvent. These values of k_{ex} are given also in Table 2. The values of k_{ex} for the salts of Cu^{2+}, Ni^{2+}, and Mn^{2+} are characteristic of strong exchange (*31*). The value of k_{ex} for $CoCl_2$ in methanol is found to be considerably lower, which probably corresponds to the transition to weak exchange (*31*). The very low value of k_{ex} for $DyCl_3$ is attributable to the small exchange integral for the screened 4*f*-electrons of Dy^{3+} (*21*).

As seen from Table 2, the product of the exchange constant (k_{ex}) with the octanol/water partition coefficient (K_p) parallels the relative values of $\Delta(1/P)$ for Cu^{2+}, Ni^{2+}, Co^{2+}, and Dy^{3+} chlorides and for Ni^{2+} salts with different counterions (cf. Figs. 1 and 2, respectively). Thus, the low value of $\Delta(1/P)$ for $CoCl_2$, compared with $NiCl_2$ and $CuCl_2$, can be explained by the relatively low values of k_{ex} for a collisional exchange interaction, rather than by a very short $T_{1,R}$ in terms of the static dipolar relaxation mechanism (cf. Table 1). Similarly, the very low value of $\Delta(1/P)$ for $DyCl_3$ is evidently explained by the low value of the exchange rate constant. Potassium ferricyanide almost does not partition into octanol, so its rather low values of $\Delta(1/P)$ may be explained partly by its low solubility in membranes.

Thus, to within the limitations of this model system, the relative values of the exchange rate constants and partition coefficients for different paramagnetic salts in organic solvent do not contradict a relaxation mechanism that is mediated by partition of the paramagnetic ions into membranes, most probably as cation–anion pairs. This is especially the case for the perchlorates, which have relatively high partition coefficients. For the remaining salts with lower partition coefficients, other mechanisms may also make a significant contribution to the overall relaxation rate.

Dependence on Ion Magnetic Moment

The static dipolar relaxation mechanism predicts a strong (quadratic) dependence of the relaxation enhancement on the magnetic moment or spin of the paramagnetic ion (see Eqs. [4], [7], [8]). On the other hand, the spin exchange rate for strong exchange between the radical and paramagnetic ion is virtually independent of the magnetic moment of the paramagnetic ion (*31*). Therefore, to discriminate between these two relaxation mechanisms it was important to compare the values of $\Delta(1/P)$ for ions which differ mainly in their electron spin. Mn^{2+} and Cu^{2+} ions are appropriate for this purpose because their spin values are $S_R = 5/2$ and 1/2, respectively, and the *g*-factors differ somewhat (see above), whereas the spin–lattice relaxation times are both on the order of 10^{-9} s (*37*).

The second integrals of the EPR spectra from Mn^{2+}-ion-containing samples are difficult to measure because of the baseline associated with the strong underlying Mn^{2+} EPR signal. For this reason, saturation curves for Mn^{2+}-containing samples were measured by using the spectral amplitude of the central hyperfine component and a linear baseline correction over this region. Microwave saturation curves were measured for 8-PCSL and 12-PCSL in DMPC membranes, in the presence of 10 mM $MnCl_2$, $MnSO_4$, or $CuCl_2$. (Lower concentrations were used in this case to reduce the amplitude of the background Mn^{2+} EPR signal). The data for the 8-PCSL spin label in fluid-phase membranes are given in Fig. 3. It is seen that the extent of saturation is lower in the presence of Cu^{2+} than in the presence of Mn^{2+}. The saturation curves for the

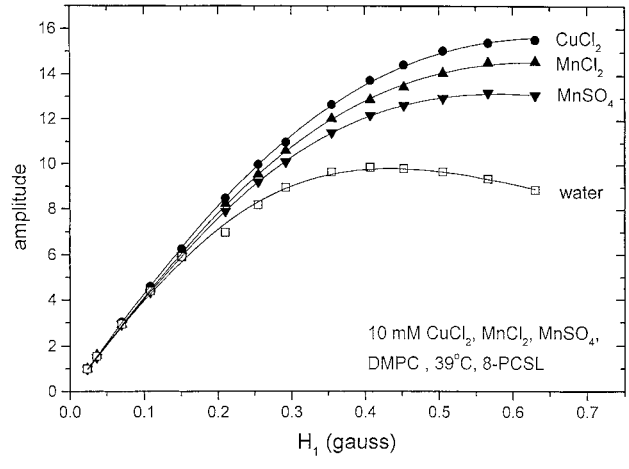

FIG. 3. Saturation curves as a function of H_1-microwave field strength for the amplitude of the central ($m_I = 0$) manifold in the EPR spectrum of 8-PCSL in DMPC membranes that are suspended in water (□), 10 mM $MnSO_4$ (▼), 10 mM $MnCl_2$ (▲), and 10 mM $CuCl_2$ (●). Temperature: 39°C.

TABLE 3

Values of $\Delta(1/P_2)$ and Corresponding Spin–Lattice Relaxation Rate Enhancements, $\Delta(1/T_1)$, and Paramagnetic Line Broadening ($\Delta\Delta\omega$) for the EPR Spectra of *n*-PCSL Spin Labels in DMPC Membranes in the Presence of 10 mM Concentrations of Mn^{2+} and Cu^{2+} Ion Salts in the Aqueous Phase

n-PCSL	T (°C)	Paramagnetic salt	$\Delta(1/P_2)$ (G^2)[a]	$\Delta(1/T_1) \times 10^{-6}$ (s^{-1})	$\Delta\Delta\omega \times 10^{-6}$ (s^{-1})[b]
5	39	$MnSO_4$	0.57	3.8 ± 0.4	7.6 ± 0.6
8	39	$MnSO_4$	0.19	1.5 ± 0.1	5.2 ± 0.3
		$MnCl_2$	0.30	2.3 ± 0.2	6.5 ± 0.3
		$CuCl_2$	0.41	3.3 ± 0.3	4.7 ± 0.3
12	39	$MnSO_4$	0.25	2.1 ± 0.2	5.9 ± 0.3
		$MnCl_2$	0.415	4.0 ± 0.4	8.4 ± 0.6
		$CuCl_2$	0.275	2.9 ± 0.3	4.1 ± 0.3
5	19	$MnSO_4$	0.1	0.74 ± 0.08	9.7 ± 0.7
8	19	$MnSO_4$	0.03	0.09 ± 0.01	5.9 ± 0.3
		$MnCl_2$	0.05	0.26 ± 0.03	7.3 ± 0.3
		$CuCl_2$	0.09	0.47 ± 0.05	4.4 ± 0.3
12	19	$MnSO_4$	0.08	0.40 ± 0.05	5.3 ± 0.3
		$MnCl_2$	0.15	1.0 ± 0.1	7.3 ± 0.3
		$CuCl_2$	0.05	0.28 ± 0.03	4.1 ± 0.4

[a] Values of $\Delta(1/P_2)$ are obtained from fitting progressive saturation curves for spin-labeled membranes in the presence and absence of paramagnetic ions to Eq. [17], yielding values of P_2 and P_2^o, respectively, where $\Delta(1/P_2) = 1/P_2 - 1/P_2^o$, with an average rmsd of 0.05 G^2. Values of $\Delta(1/T_1)$ are obtained from spectral simulations (see text).

[b] Peak-to-peak linewidths ΔH^{PP} and ΔH_o^{PP} are measured for the central line ($m_I = 0$) in the low-power EPR spectrum, in the presence and absence of paramagnetic salt, respectively. Expressed in angular frequency units, the T_2-relaxation enhancement is $\Delta\Delta\omega = (\sqrt{3}/2)\gamma_e(\Delta H^{PP} - \Delta H_o^{PP})$.

spectral amplitude, A, could be fitted satisfactorily to the following semi-empirical expression:

$$A = \frac{A_o \cdot H_1}{(1 + P_2 \cdot H_1^2)^{\epsilon}}, \qquad [17]$$

where the parameter P_2 is similar to the saturation parameter P characterizing the saturation of the double integral of the spectral intensity (see Eq. [1]). The values of the exponent, ϵ, in Eq. [17] lie in the ranges 1.38–1.5 and 1.15–1.2 at 19 and 39°C, respectively, for 5-, 8-, and 12-PCSL in DMPC membranes. These exponents remained approximately the same in the presence and absence of paramagnetic salts.

The values of $\Delta(1/P_2)$ for 8-PCSL and 12-PCSL in the presence of 10 mM $MnCl_2$, $MnSO_4$, or $CuCl_2$ are given in Table 3. For 8-PCSL, the smaller values of $\Delta(1/P_2)$ for $MnCl_2$ relative to $CuCl_2$, e.g., 0.30 versus 0.41 G^2 in the fluid phase, are contrary to expectations for a static dipolar relaxation mechanism (cf. Table 1). They are, however, consistent with a collisional spin exchange mechanism because the octanol partition coefficient (and to a lesser extent the value of k_{ex}) is lower for $MnCl_2$ than for $CuCl_2$ (see Table 2). In the case of 12-PCSL, the relative values of $\Delta(1/P_2)$ for $MnCl_2$ and $CuCl_2$ are in the direction expected for a dipolar relaxation enhancement, but their ratio is much less than that predicted from the relative values of $T_{1,dd}^{-1}$ (static) in Table 1.

The saturation curve for 8-PCSL in DMPC in the presence of 10 mM $MnSO_4$ corresponds to a higher degree of saturation (i.e., lower value of $\Delta(1/P_2)$) than that with $MnCl_2$ (see Fig. 3). A similar trend is found also for measurements with 12-PCSL (see Table 3). As for $NiSO_4$ (Table 2), $MnSO_4$ partitions less into octanol (and, hence, into the membrane) than does the corresponding chloride. Therefore the lower values of $\Delta(1/P_2)$ for $MnSO_4$ correspond to lower partitioning into the membrane compared with the chloride, which is similar to the case with the corresponding Ni^{2+} salts.

Thus, all of the experimental results obtained, with the possible exception of the sulfate salts, indicate that the relaxation enhancements produced by different paramagnetic ions in the fluid phase of DMPC or egg PC membranes are caused substantially by partitioning of these ions into the membrane, most probably as ion pairs. The principal contribution to the relaxation enhancement is then a collisional spin exchange interaction, or a dipole–dipole interaction (possibly dynamic), with the spin labels. The relaxation enhancement obtained with the sulfate salts, which have the lowest partition coefficients, gives an upper limit for the static dipolar contribution from paramagnetic ions confined to the aqueous phase or to the membrane surface.

Analysis of Low-Power Spectra

Because of the possibility that paramagnetic species penetrate the membrane, evidence for spin–spin interactions was also sought from the conventional EPR lineshapes. The linear (i.e., nonsaturated) EPR spectra of the membrane-incorporated *n*-PCSL spin labels, in the presence of paramagnetic salts, were used to determine the additional Lorentzian line broadening relative to membrane samples in water. This additional broadening was absent in the presence of diamagnetic $MgCl_2$ (the ionic radius of Mg^{2+} is close to those of Ni^{2+}, Cu^{2+}, and Co^{2+} (*38*)). For 5-PCSL and 8-PCSL in fluid DMPC and egg PC membranes, the paramagnetic broadening is rather significant in the presence of Cu^{2+} and Ni^{2+} perchlorates and chlorides (see, e.g., Fig. 4). The values of the paramagnetic broadening were determined from spectral simulations and also directly by measuring the peak-to-peak linewidth of the central ($m_I = 0$) spectral component or the half-width at half-height of the low-field ($m_I = +1$) component. Values of the spin–spin relaxation enhancements ($\Delta\Delta\omega$) estimated from the paramagnetic broadening of the $m_I = 0$ hyperfine component, by using the relation for Lorentzian lineshapes, $\Delta\Delta\omega = (\sqrt{3}/2)\gamma_e\Delta\Delta H^{PP}$, are given in Fig. 5 for various *n*-PCSL spin labels in fluid DMPC membranes in the presence of $CuCl_2$, $Ni(ClO_4)_2$, or $NiCl_2$. The relative values of the line broadening for $CuCl_2$ and $NiCl_2$ and the dependence on spin-label position, *n*, are seen to correlate with the corresponding values of

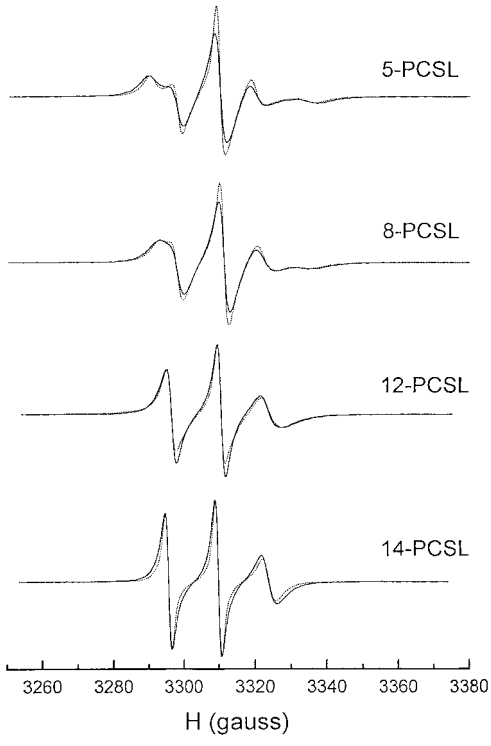

FIG. 4. EPR spectra of *n*-PCSL phosphatidylcholine spin labels in DMPC membranes at 39°C, in the presence (solid lines) and absence (dotted lines) of 30 mM $Ni(ClO_4)_2$. From top to bottom, spectra are of 5-PCSL, 8-PCSL, 12-PCSL, and 14-PCSL.

$\Delta(1/P)$ (cf. Fig. 1). It is found that the line broadening is largest for Cu^{2+} and Ni^{2+} perchlorates, is very small for Co^{2+} and Dy^{3+} chlorides, and is absent for magnesium chloride, which was used as a control.

The paramagnetic broadenings, $\Delta\Delta\omega$, of the $m_I = 0$ components in the spectra of 8-PCSL and 12-PCSL in fluid DMPC membranes, which are induced by 10 mM $MnCl_2$, $MnSO_4$, or $CuCl_2$, are given in Table 3. For both spin labels, these values are greater in the presence of $MnCl_2$ than the corresponding values in the presence of $CuCl_2$. However, this difference is less than a factor of 10–20 times that is predicted for a static dipolar interaction (cf. Table 1). At the same time, the values of $\Delta\Delta\omega$ for Mn^{2+} ions depend on the nature of the counterion: they are greater for $MnCl_2$ than for $MnSO_4$.

Spin-Label T_1 Relaxation Times

Absolute values of T_1 and $T_{1,o}$, and hence of the spin–lattice relaxation enhancements $\Delta(1/T_1)$, were obtained from simulations of the partially saturated spectra. The model used for simulation was one of spin-label rotational diffusion within a cone with allowance for microwave saturation and the Zeeman field modulation. Calibrations were established for the experimental values of the saturation parameters, P and P_2, for the integrated intensities (Eq. [1]) and spectral amplitudes (Eq. [17]), respectively. The dynamic parameters (cone angle γ or order parameter, S_{zz}, and the rotational correlation time, τ_R) and spectral parameters (intrinsic spin–spin relaxation time, T_2, and inhomogeneous Gaussian broadening, ΔH_G) were first determined from simulations of the corresponding linear (i.e., low power) EPR spectra. Full details of the model and calibrations for the relaxation parameters obtained from simulations will be given elsewhere. Limitations on the accuracy in determining the T_1 values from such simulations come from the approximations of the motional model, as well as from the difficulty in extracting intrinsic T_2 values from inhomogeneously broadened lineshapes. In particular, simulations of the linear EPR spectra were found to be only approximate for 12-PCSL and 16-PCSL in the gel phase. However, the enhancements (i.e., differences) in relaxation rates $\Delta(1/T_1)$ and $\Delta(1/T_2)$ were found to be relatively insensitive to the exact values of the simulation parameters. The values of $\Delta(1/T_1)$ for different paramagnetic ions and different *n*-PCSL spin labels are given in Table 4. Values of the paramagnetic broadening ($\Delta\Delta\omega \equiv \Delta\Delta(1/T_2)$) deduced from simulations of the linear (i.e., nonsaturated) spectra are also given in Table 4 for the same systems.

The enhancements in T_1-relaxation rate obtained by this nonlinear CW method are comparable to those obtained from time-domain saturation recovery techniques. For instance, a value of $\Delta(1/T_1) = 1.4 \times 10^6\ s^{-1}$ was measured for 9-PCSL in DOPC–cholesterol membranes in the presence of 50 mM $K_3Fe(CN)_6$ by saturation recovery (*39*). Using the present technique and data from Fig. 1, a value of $\Delta(1/T_1) = 1 \times 10^6$

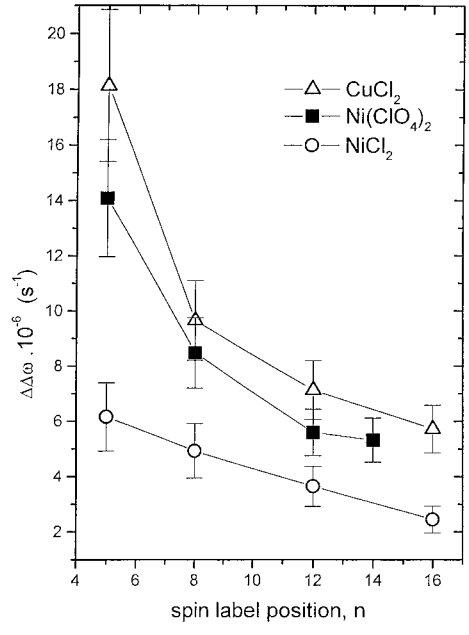

FIG. 5. Dependence of the additional broadening, $\Delta\Delta\omega$, of the central ($m_I = 0$) spectral manifold of *n*-PCSL in DMPC at 39°C on spin-label position, *n*, in the presence of 30 mM $CuCl_2$ (△), 30 mM $Ni(ClO_4)_2$ (■), or 30 mM $NiCl_2$ (○).

TABLE 4

Spin–Lattice Relaxation Enhancements, $\Delta(1/T_1)$, and Paramagnetic Line Broadening ($\Delta\Delta\omega$) for Spin-Labeled Phospholipids *n*-PCSL in Fluid DMPC Membranes in the Presence of 30 mM Paramagnetic Ion Salts[a]

Spin label	Paramagnetic salt	$\Delta(1/T_1) \times 10^{-6}$ (s^{-1})	$\Delta\Delta\omega \times 10^{-6}$ (s^{-1})
5-PCSL	$NiCl_2$	4.6 ± 0.4	5.3 ± 0.4
	$CuCl_2$	8.8 ± 0.4	12.3 ± 0.4
	$Ni(ClO_4)_2$	14.0 ± 0.4	13.6 ± 0.4
8-PCSL	$NiCl_2$	3.9 ± 0.4	4.4 ± 0.4
	$CuCl_2$	5.1 ± 0.4	8.8 ± 0.4
	$Ni(ClO_4)_2$	10.6 ± 0.4	11.4 ± 0.4
12-PCSL	$NiCl_2$	2.4 ± 0.4	2.6 ± 0.4
	$Ni(ClO_4)_2$	8.7 ± 0.4	8.8 ± 0.4
14-PCSL	$Ni(ClO_4)_2$	7.0 ± 0.4	7.0 ± 0.4
16-PCSL	$NiCl_2$	3.5 ± 0.4	2.6 ± 0.4
	$CuCl_2$	3.2 ± 0.4	7.9 ± 0.4

[a] Obtained from spectral simulations, where the T_2-relaxation enhancement, $\Delta\Delta\omega$, is obtained from the Lorentzian half-widths at half-height of the low-field ($m_I = +1$) manifold. $T = 39°C$.

s^{-1} is found for 8-PCSL in DMPC membranes at 39°C in the presence of 30 mM $K_3Fe(CN)_6$.

It is seen from Table 4 that, in the presence of Ni^{2+} chlorides and perchlorates, the values of $\Delta\Delta\omega$ and $\Delta(1/T_1)$ measured for several spin labels are close to one another. However, in the case of Cu^{2+} ions, the values of $\Delta\Delta\omega$ are systematically larger than those of $\Delta(1/T_1)$ for all spin labels.

The spin–lattice relaxation enhancements $\Delta(1/T_1)$ for 5-PCSL, 8-PCSL, and 12-PCSL that are induced by the presence of 10 mM $MnCl_2$, $MnSO_4$, or $CuCl_2$ were also determined from spectral simulations in terms of the P_2 saturation parameter of Eq. [17] for the spectral amplitude. These values are included in Table 3. In the fluid phase, the values of $\Delta(1/T_1)$ are lower than the corresponding values of $\Delta\Delta\omega$ in Table 3 for all three paramagnetic salts, the ratio $\Delta(1/T_1)/\Delta\Delta\omega$ being higher for $CuCl_2$ than for $MnCl_2$ and $MnSO_4$.

Dependence on Lipid Phase

The temperature dependence of both the paramagnetic broadening and the effects of paramagnetic relaxation on the saturation behavior were also measured. Values of $\Delta(1/P)$ for 8-PCSL and 16-PCSL in DMPC membranes in the presence of $NiCl_2$ are given as a function of temperature in Fig. 6. The temperature dependence is relatively slight in the gel phase. It increases at the lipid chain-melting transition (ca. 23°C) and continues to increase rather steeply in the fluid phase (at least for 8-PCSL).

The DMPC membrane becomes thinner at the chain-melting transition and continues to thin with increasing temperature in the fluid phase (*12, 40*). The increase in paramagnetic enhancement of membrane-embedded spin labels is therefore in qualitative agreement with expectations for a static dipolar interaction with ions confined to the aqueous phase. However, much of the evidence given above points to a major contribution to the relaxation enhancement in the fluid phase from partitioning of the paramagnetic ions into the membrane. The temperature dependence observed is consistent with such an interpretation, because it is expected that partitioning into the membrane will increase at the chain-melting transition and that both partitioning and frequency of collision with the spin label will increase with increasing temperature in the fluid phase.

Effects of Membrane Composition

Because of the importance of paramagnetic ion partitioning into the membrane, it is of interest to explore the effects that membrane lipid composition has on the paramagnetic relaxation enhancement and broadening. For the *n*-PCSL spin labels in egg PC membranes, the dependence of $\Delta(1/P)$ on *n* is given in Fig. 7. It is seen that the *n*-dependences in egg PC are qualitatively similar to those for fluid DMPC membranes (Fig. 1), although differences in the detailed profile are observed. The largest discrepancy between the profiles is at the C-8 position, which is close to the location of the *cis*-double bond in the oleoyl *sn*-2 chain of egg PC. A rather strong dependence of the $\Delta(1/P)$ parameters on the counterion is also observed for egg PC membranes (Fig. 7), just as for fluid DMPC membranes (Fig. 2).

Inclusion of cholesterol in the egg PC membranes gives rise to pronounced changes in the dependence of $\Delta(1/P)$ on spin

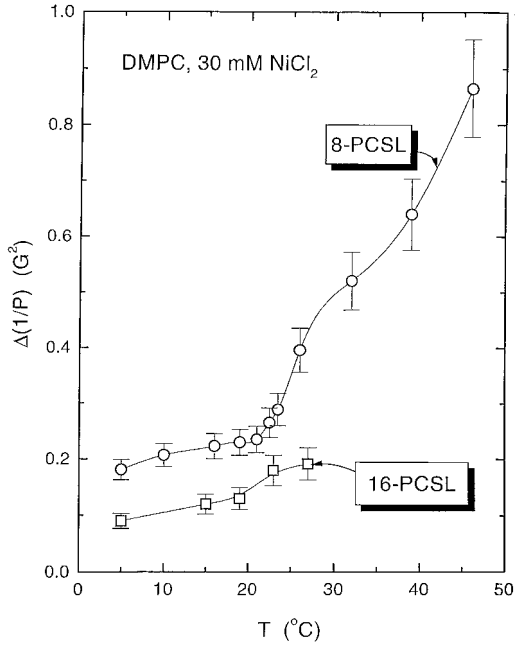

FIG. 6. Temperature dependences of the $\Delta(1/P)$ relaxation enhancement parameter for 8-PCSL (○) and 16-PCSL (□) in DMPC membranes in the presence of 30 mM $NiCl_2$.

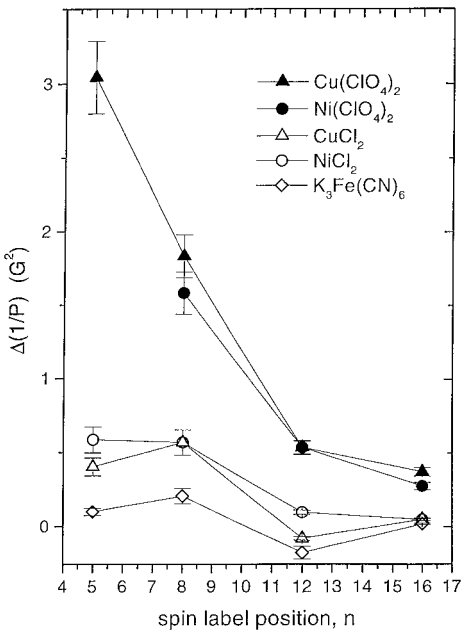

FIG. 7. Dependence of the $\Delta(1/P)$ relaxation enhancement parameter on spin-label position, n, for n-PCSL in egg phosphatidylcholine membranes at 39°C, in the presence of chlorides and perchlorates of Ni^{2+} and Cu^{2+} at a bulk concentration of 30 mM: $CuCl_2$ (△), $NiCl_2$ (○), $Cu(ClO_4)_2$ (▲), $Ni(ClO_4)_2$ (●), and for $K_3Fe(CN)_6$ (◇).

label position, as is shown in Fig. 8. In the presence of 30 mol% cholesterol, the value of $\Delta(1/P)$ for 5-PCSL positioned in the more polar part of the bilayer increases, whereas that for 16-PCSL located toward the hydrophobic centre of the bilayer decreases. This striking modification of the relaxation enhancement profile allows conclusions to be drawn about the nature of divalent cation permeation into the membrane (see later Discussion).

$P_{\beta'}$ Gel Phase

The dependences of the $\Delta(1/P)$ parameter and paramagnetic broadening of the linear EPR spectra on spin-label position (n) were also studied in the intermediate $P_{\beta'}$ gel phase, in a way similar to that for the liquid crystalline L_α-phase, and for both different paramagnetic ions and different counterions. It is found that: (1) The values of $\Delta(1/P)$ and $\Delta(1/P_2)$ are significantly smaller than for the fluid phase. (2) The dependence of $\Delta(1/P)$ on spin-label position for different ions (including Mn^{2+}) is rather weak and nonmonotonic. In particular, for some ions (Ni^{2+} and Co^{2+}), a small but distinct maximum exists in the region of the C-8–C-10 positions. (3) A dependence of $\Delta(1/P)$ and $\Delta(1/P_2)$ on the nature of the anion is also observed in the $P_{\beta'}$ intermediate gel phase for Ni^{2+} and Mn^{2+} ions (see Table 3). (4) There is no complete correlation between the values of $\Delta(1/T_1)$ and $\Delta\Delta\omega$ (see Table 3).

The values of $\Delta(1/T_1)$ for 5-PCSL, 8-PCSL, and 12-PCSL in DMPC in the presence of 10 mM $CuCl_2$, $MnCl_2$, or $MnSO_4$ at 19°C are given in Table 3. It is seen that the spin–lattice relaxation enhancements in the $P_{\beta'}$ gel phase are considerably lower than in the fluid phase; furthermore, the former values are an order of magnitude smaller than the corresponding values of $\Delta\Delta\omega$ in Table 3. At the same time there is a dependence of $\Delta(1/T_1)$, $\Delta\Delta\omega$ and $\Delta(1/P_2)$ on the nature of the anion.

Diamagnetic $MgCl_2$ and $Mg(ClO_4)_2$ were used as controls also in the $P_{\beta'}$ intermediate gel phase. The values of $\Delta(1/P_2)$ for 8-PCSL in the presence of 30 mM $MgCl_2$ and of 5-PCSL in the presence of 30 mM $Mg(ClO_4)_2$ were -0.03 and -0.04 G^2, respectively. In the linear EPR spectrum, a decrease in linewidth of 0.22 G for $Mg(ClO_4)_2$ and, simultaneously, an increase in the outer splitting, A_{max}, by 0.95 G was observed. Thus, the negative values of $\Delta(1/P)$ for $MgCl_2$ and $Mg(ClO_4)_2$ in the $P_{\beta'}$ intermediate gel phase, like those in the liquid crystalline phase, are due to a perturbation of the rotational dynamics, i.e., an increase in T_2^{eff}.

These results indicate that in the $P_{\beta'}$ intermediate gel phase, as well as in the liquid crystalline phase, the paramagnetic relaxation enhancements are not dominated by a static dipolar interaction of the membrane-bound spin labels with paramagnetic ions in the aqueous phase, but in an anion-dependent fashion are due to partitioning of paramagnetic ions into the membrane.

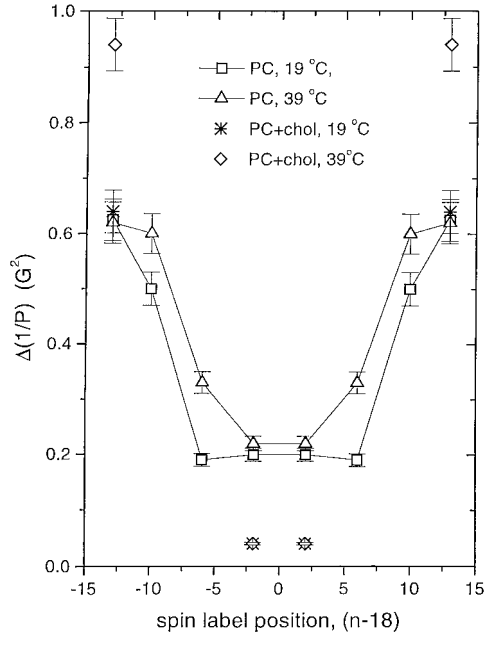

FIG. 8. Dependence of the $\Delta(1/P)$ relaxation enhancement parameter on spin-label position, n, for n-PCSL in egg phosphatidylcholine (PC) membranes with and without 30 mol% cholesterol, at 19 and 39°C. Egg PC at 19°C (□); egg PC at 39°C (△); egg PC + 30 mol% cholesterol at 19°C (✳); egg PC + 30 mol% cholesterol at 39°C (◇). In each case, relaxation is induced by 30 mM $NiCl_2$.

DISCUSSION

Besides demonstrating the different efficiencies of various paramagnetic ions for inducing spin-label relaxation enhancement, this study shows the importance of the penetration of ions into the membrane, which depends strongly on the compensating anion. To use the latter to derive spin-label positional information, both lateral and transverse, and also dynamic information on the paramagnetic ions within the membrane, it is necessary to analyze the mechanisms of relaxation enhancement and broadening. This is done in the following sections. First, intramembrane relaxation and broadening mechanisms are considered. It is shown that dipolar mechanisms do not contribute greatly to the intramembrane interactions with dissolved paramagnetic ions, in the case of Ni^{2+}, but may be appreciable in the case of Cu^{2+} and Mn^{2+}. Then, the intramembrane spin exchange frequencies are used to investigate translational diffusion of the paramagnetic ions. Finally, the dependence on membrane composition is used to deduce salient features of the divalent ion permeation mechanism.

Intramembrane Spin Exchange and Dipolar Interactions

Because of the membrane penetration of the paramagnetic ions, it is necessary to estimate the relative effectiveness of both dipolar and exchange mechanisms of relaxation enhancement by interactions taking place within the membrane. In this section we consider T_1 relaxation; T_2 relaxation is dealt with later. Strong exchange holds for Ni^{2+} ions (see Table 2), and the rate of Heisenberg exchange, $T_{1,HE}^{-1}$, are given by the combination of Eqs. [2] and [13],

$$T_{1,HE}^{-1} = 4\pi\sigma_{RL}r_{RL}D_T(z)\cdot n_R(z), \qquad [18]$$

where the local ion concentration $n_R(z)$ at distance z along the membrane normal is expressed as ions per unit volume. The rate of static spin–lattice dipolar relaxation induced by paramagnetic ions located in the membrane can be expressed in terms of the integrated value,

$$\langle T_{1,dd}^{-1}\,(\text{static})\rangle = \frac{4}{3}\cdot\mu_R^2\gamma_e^2T_{1,R}\left[\int_0^d\int_{r_{RL}}^{\infty}\frac{n_R(z)2\pi\rho d\rho dz}{[(z-z_{SL})^2+\rho^2]^3} + \int_d^{2d}\int_0^{\infty}\frac{n_R(z)2\pi\rho d\rho dz}{[(z-z_{SL})^2+\rho^2]^3}\right], \qquad [19]$$

where z_{SL} is the vertical location of the spin-label group and d is the bilayer half-width. This equation is obtained from Eq. [4] by angular averaging, and the condition $\omega T_{1,R} \ll 1$ that is valid for Ni^{2+} ions is assumed. As regards the lower limit of the radial integral over ρ, it is reasonable to take the same value of r_{RL} that is used above for diffusional encounters.

For numerical evaluation of the ratio $\langle T_{1,dd}^{-1}\,(\text{static})\rangle/T_{1,HE}^{-1}$ one must specify the ion concentration profile in the membrane. We take an exponential decay (for which there is some experimental justification—see Ref. (*5*)): $n_R(z) = n_{R,0}e^{-\alpha z}$ for $0 < z < d$ and $n_R(z) = n_{R,0}e^{-\alpha(2d-z)}$ for $d < z < 2d$, where $n_{R,0}$ is the ion concentration on the lipid side of the lipid/water interface, which generally is not equal to that on the aqueous side. (It is also noted that the transmembrane polarity profile decreases progressively toward the center of the membrane.) As an estimate for $1/\alpha$ we take the distance at which the values of $\Delta(1/P)$ for $NiCl_2$ and $Ni(ClO_4)_2$ decrease e-fold. For both relaxants, this corresponds to a position between the NO groups of 5-PCSL and 14-PCSL in DMPC membranes (see Figs. 1 and 2) and therefore $1/\alpha = 0.95$–1.15 nm (see, e.g., (*41*)). Taking $r_{RL} \approx 0.45$ nm (*42*, *43*) then: $\langle T_{1,dd}^{-1}\,(\text{static})\langle/T_{1,HE}^{-1} = B_1/D_T$, where the factor $B_1 \approx 5$–8×10^{-8} cm^2 s^{-1} for $z_{SL} = 0.8$–2.2 nm. Thus, the Heisenberg exchange mechanism dominates for translational diffusion coefficients $D_T > 5$–8×10^{-8} cm^2 s^{-1}.

In the case of rapid translational diffusion, effective spin-label T_1 relaxation may also be induced by the dynamic dipolar mechanism, but only by ions with g-values close to that of the spin label. In the latter case we have, from Eq. [16],

$$T_{1,dd}^{-1}\,(\text{dynamic}) = (4\pi/15^2)\mu_R^2\gamma_e^2n_R/(D_Tr_{RL}). \qquad [20]$$

Then with Mn^{2+}, which is the only ion studied for which the g-value is close to that of the spin label, $T_{1,dd}^{-1}\,(\text{dynamic})/T_{1,HE}^{-1} \approx 2.0 \times 10^{-12}$ cm^4 s^2/D_T^2 and Heisenberg exchange dominates over dynamic dipolar relaxation for diffusion coefficients $D_T > 2 \times 10^{-6}$ cm^2 s^{-1}. As might be anticipated, this condition requires faster translational diffusion rates than for that in which collisional exchange dominates static dipolar relaxation.

Comparison with Experiment

Values of the translational diffusion coefficient for divalent ions, estimated from their values in water (*38*) by using the Stokes–Einstein relation, are $D_T = 5 \times 10^{-7}$–10^{-7} cm^2 s^{-1} for effective membrane viscosities of 20 to 100 cP, respectively. In comparison, the anomalous non-Stokesian diffusion coefficients found for small polar nonelectrolytes in liquid hydrocarbons and in polymers reach values of up to $D_T = 3 \times 10^{-5}$ cm^2 s^{-1} (*40*–*46*). Thus, using these estimates for the translational diffusion coefficients of divalent ion pairs in membranes shows that for Ni^{2+} ions the Heisenberg exchange interaction should dominate over dipolar relaxation.

Experimental arguments in favor of the Heisenberg exchange mechanism are the temperature dependences of the relaxation enhancements measured for Ni^{2+} chlorides and perchlorates (see, e.g., Fig. 6). Diffusion in the membrane is an activated process and one expects the Heisenberg exchange rate to increase with increasing temperature, as is observed experimentally. On the other hand, dynamic dipolar relaxation

becomes less effective with increasing D_T and for a static mechanism, with the condition $\omega T_{1,R} \ll 1$, one would expect either no temperature dependence or rather a decrease in $T_{1,dd}^{-1}$ because $T_{1,R}$ is expected to decrease with increasing temperature (see Eqs. [19] and [20]). It should be noted, however, that the paramagnetic ion concentration in the membrane may increase with temperature, thus increasing the contributions from both exchange and dipolar relaxation mechanisms. If, conversely, the paramagnetic ion concentration in the membrane were to decrease with increasing temperature, the dipolar mechanism would definitely be excluded.

Similar arguments and conclusions are (most probably) valid for the fast-relaxing Co^{2+} ions for which, however, the rate constants for Heisenberg-exchange, octanol partition coefficients and, correspondingly, the values of $\Delta(1/P)$ and $\Delta\Delta\omega$ (and $\Delta(1/T_1)$) are significantly smaller than for Ni^{2+} ions. For the slower relaxing Cu^{2+} and Mn^{2+} ions, there is a greater possibility of appreciable enhancements from dipolar interactions. This latter case requires consideration of T_2 relaxation for which dipolar mechanisms are more effective.

Dipolar T_2 Relaxation and Line Broadening

For Heisenberg exchange interactions, the contribution to the spin-label T_2 relaxation is equal to the contribution to T_1 relaxation. For magnetic dipole–dipole interactions, on the other hand, the T_2-relaxation enhancement is greater in general than that for T_1 relaxation (compare Eqs. [7]–[9] with Eqs. [10]–[12] and Eq. [14] with Eq. [16]). Only in the case of extreme narrowing, $\omega^2 T_{1,R}^2 \ll 1$ (i.e., only for Ni^{2+} and Co^{2+}) is T_{2dd}^{-1} (static) $= T_{1dd}^{-1}$ (static), for the static contribution to dipolar relaxation (cf. Table 1). It is seen from Table 4 that, in the presence of Ni^{2+} ions, the enhancement in T_2 relaxation, $\Delta\Delta\omega$, is approximately equal to that in T_1 relaxation, $\Delta(1/T_1)$. For Ni^{2+} ions, paramagnetic relaxation enhancement is therefore dominated by Heisenberg exchange. Static dipolar enhancements that would contribute equally to T_1 and T_2 relaxation, in this case, have already been estimated to be less significant. However, for Cu^{2+} ions and also for Mn^{2+} ions (see Tables 3 and 4), the values of $\Delta\Delta\omega$ are greater than those of $\Delta(1/T_1)$, indicating an appreciable contribution from dipolar paramagnetic broadening.

For 30 mM Cu^{2+} ions, $\Delta\Delta\omega$-$\Delta(1/T_1) \approx 3$–$4 \times 10^6\ s^{-1}$ (see Table 4). This difference is comparable to the T_2 enhancement from static dipolar interactions with surface-absorbed Cu^{2+} ions that was estimated above by using modified Leigh theory (see Table 1). However, abundant experimental evidence was given above for the penetration of Cu^{2+} ions—most probably as ion pairs—into the membrane interior, at least for the perchlorate salt. Intramembrane dipolar interactions are therefore expected to make an appreciable contribution to the relaxation enhancement by Cu^{2+} ions. This can arise from modulation of the dipolar interaction by spin–lattice relaxation of the paramagnetic ion (the static case) or by translational diffusion of the paramagnetic ions (the dynamic case).

The contribution to the T_2 enhancement from dynamic dipolar relaxation, $T_{2,dd}^{-1}$ (dynamic), is given by Eq. [15]. The contribution to T_2 relaxation from dipolar interactions modulated by the paramagnetic ion spin–lattice relaxation, $T_{2,dd}^{-1}$ (static), can be estimated in a way analogous to that used for the static contribution to T_1 relaxation (cf. Eq. [19]). However, the lower integration limit, r_{RL}, must be modified if the dipolar interactions become so large, on close approach, that they are no longer averaged by T_1 relaxation of the metal ion. The condition for this is that $\gamma_e \mu_R / r_c^3 \approx T_{1,R}^{-1}$, which corresponds to a critical distance of $r_c = 0.7$ nm for Cu^{2+} ions. With $1/\alpha \approx 0.85$ nm, as deduced from the data for $CuCl_2$ in Fig. 1, the ratio of the transverse relaxation rates from the two mechanisms is then $T_{2,dd}^{-1}$ (dynamic)/$T_{2,dd}^{-1}$ (static) $= B_2/D_T$, where $B_2 = 0.3$–$2 \times 10^{-6}\ cm^2\ s^{-1}$ for z_{SL} in the range 2.2–0.8 nm. Thus the motional mechanism of dipolar T_2 relaxation dominates if the translational diffusion coefficient of the Cu^{2+} ion pairs is greater than $2 \times 10^{-6}\ cm^2\ s^{-1}$. This relatively high value suggests that both dipolar mechanisms may make appreciable contributions to the T_2 enhancement.

For Mn^{2+} ions, it follows from the experimental values of $\Delta\Delta\omega$ and $\Delta(1/P_2)$ (Table 3), and from estimates of the static dipolar enhancements (Table 1), that ions adsorbed at the membrane surface can contribute not only to the $\Delta(1/T_2)$ rate enhancement but also to the value of $\Delta(1/T_1)$. Thus, as seen from Table 3, the relative differences in $\Delta(1/P_2)$ values for $CuCl_2$ and $MnCl_2$ are less than those in the corresponding exchange-partition coefficient products, $K_p \cdot k_{ex}$ (cf. Table 2). The values of $\Delta\Delta\omega$ for 8-PCSL in the presence of 10 mM $MnCl_2$ are close to the static dipolar estimates for $T_{2,dd}^{-1}$ (Table 1) and are greater (although by less than 10 times) than the corresponding values for $CuCl_2$ (see Table 3). However, the values of $\Delta(1/P_2)$ and $\Delta\Delta\omega$ for Mn^{2+}, as those for Ni^{2+} and Cu^{2+} ions, depend on the nature of the counterion. They are greater for $MnCl_2$ compared with $MnSO_4$ (see Table 3). Also, the values of $\Delta(1/P_2)$ in the presence of Cu and Mn chlorides are comparable in magnitude: for 8-PCSL they are greater in the presence of Cu^{2+} and for 12-PCSL they are greater in the presence of Mn^{2+} (see Table 3). These data show that, in the case of Mn^{2+}, the dipolar interactions both with ions in the aqueous phase and with paramagnetic ions partitioned into the membrane contribute to the net $T_{1,dd}^{-1}$ and $T_{2,dd}^{-1}$ relaxation rate enhancements.

In the $P_{\beta'}$ intermediate gel phase, the paramagnetic line broadening is of the same order of magnitude as in the fluid phase, whereas the ratios $\Delta(1/T_1)/\Delta\Delta\omega$ are significantly lower than the corresponding values for the fluid phase, both for Cu^{2+} and Mn^{2+} ions (see Table 3). These results indicate that the contribution of Heisenberg exchange to the T_2-relaxation enhancement is very small in the $P_{\beta'}$ phase, evidently because of the slower translational dynamics in the gel state. For the same reason, a purely static dipolar interaction appears to dominate over the dynamic (or diffusion-controlled) dipolar relaxation. In favor of this argument is the rather small difference between

the values of the paramagnetic broadening at 19 and 39°C for Mn^{2+} and Cu^{2+} ions (see Table 3).

Thus, all the experimental results obtained allow one to conclude that the relaxation enhancements produced by different paramagnetic ions in the liquid crystalline and $P_{\beta'}$ phases of DMPC, and in egg PC membranes, are caused to a considerable extent by partitioning of these ions into the membrane—most probably as ion pairs—and the resulting Heisenberg exchange or dipole–dipole interactions with the spin labels.

Intramembrane Translational Diffusion

The Smoluchowski expression for the diffusion-controlled rate constant of collision between paramagnetic ion and spin label in the membrane is given by Eq. [13] above. Using the corresponding Eq. [18] with $\sigma_{RL} = 1$ gives an upper limit for the product of the translational diffusion coefficient and the average (local) ion concentration in the membrane, when it is assumed that dipolar interactions are negligible. If one takes an encounter radius of $r_{RL} \approx 0.5$ nm (*42, 43*), then for $\Delta\Delta\omega = 5.3 \times 10^6\ s^{-1}$ (corresponding to an additional broadening of 0.3 G) one obtains $D_T n_R \approx 8.4 \times 10^{12}\ cm^{-1}\ s^{-1}$, where the intramembrane ion concentration n_R is given in cm^{-3}.

The diffusion coefficients for divalent ions in lipid membranes are not known. Values for the diffusion coefficients of the hydrated ions in water are around $D_T \approx 10^{-5}\ cm^2\ s^{-1}$ (*38*). Taking this value of D_T gives a lower estimate for the concentration of ion pairs in the membrane of $n_R \approx 8.5 \times 10^{17}\ cm^{-3}$, which corresponds to a molar intramembrane concentration of $c_i \geq 1.4$ mM. Using even a conservative estimate of the effective intramembrane viscosity of $\eta_M \approx 20$ cP (*47*) would increase this value by a factor of 20, according to the Stokes–Einstein relation. It therefore seems likely that the intramembrane diffusion of the divalent ions takes place by some mechanism other than the simple viscosity dependence predicted by the Stokes–Einstein model.

It is therefore of interest to compare the present results on divalent paramagnetic ions with data on diffusion of small polar nonelectrolytes and gases (O_2) in membranes and polymers (*44–46*). For these molecules, anomalously high diffusion is known to occur (*44, 45*) with translational diffusion coefficients in polymers and liquid hydrocarbons reaching values of $D_T \approx 3 \times 10^{-5}\ cm^2\ s^{-1}$. The mechanism of such anomalous diffusion is thought to be connected with structural defects in these cases (*44*).

The relaxation enhancement produced by Heisenberg spin exchange interactions of molecular oxygen with spin labels in membranes was studied in detail by Hyde and co-workers (*48, 49*). The concentration-diffusion product was found to be about $D_T n_R \approx 10^{13}\ cm^{-1}\ s^{-1}$ in the fluid phase of DMPC membranes. This value is of the same order of magnitude as the $D_T n_R$ product found here for Cu^{2+} and Ni^{2+} perchlorates and chlorides in fluid lipid membranes. However, the $D_T n_R$ product for O_2 decreases by an order of magnitude at the main phase transition (*48, 49*), in contrast to the approximately twofold decrease found here for $\Delta(1/P)$ (Fig. 6). The apolar oxygen molecule has greater affinity for the hydrophobic region of membrane, and its fast diffusion is attributed to the movement of small conformational defects (of a kink type) in the bulk lipid (*49–51*). In contrast to molecular oxygen, the 3*d* metal ions are strongly polar and therefore are probably located in other defect microregions, possibly in those where water molecules are occluded. These latter defect regions may not sense the main phase transition to such a great extent.

Effects of Membrane Composition

It is instructive to compare the dependence of $\Delta(1/P)$ or $\Delta\Delta\omega$ on spin-label position for paramagnetic ions with the corresponding dependences for oxygen transport (*49*) and membrane polarity (*52*) when changing the lipid composition. As will be seen below, this gives a strong indication of the permeation path taken by paramagnetic ions into the membrane.

Addition of 30 mol% cholesterol increases the relaxation enhancement in the polar region of the membrane and decreases it at the hydrophobic membrane midregion (Fig. 8). For oxygen transport, the opposite change is observed: cholesterol decreases the oxygen transport parameter in the polar region and increases it in the middle of the bilayer (*49*). On the other hand, there is a good correlation of the changes in $\Delta(1/P)$ for paramagnetic ions with the polarity changes produced by cholesterol that were observed using *n*-PCSL spin labels in lipid membranes (*52*). Intercalation of cholesterol (50 mol%) increases the polarity in the more polar region of the bilayer but decreases it in the central hydrophobic region of the bilayer. Thus, probably, paramagnetic metal ions are located in the membrane in the same regions as those in which penetrant water molecules are occluded.

CONCLUSIONS

Different relative contributions from the various mechanisms of spin-label relaxation enhancement in fluid membranes are found depending on the paramagnetic salt. Experimental design may therefore be optimized to the particular situation by the appropriate choice of relaxation agent. With the exception of Co^{2+}, the efficiency of relaxation enhancement by Heisenberg spin exchange at a fixed concentration is comparable for all 3*d* ions studied. The strength of the enhancement depends also on the solubility of the ion in the membrane, which is controlled principally by the anion. Relaxation by dipolar interactions is strongest for paramagnetic ions with longer T_1 values, Cu^{2+} and Mn^{2+}, of which Mn^{2+} is more effective because of its higher electron spin.

For experiments relying solely on Heisenberg exchange interactions, Ni^{2+} is the paramagnetic ion of choice with fluid membranes, because complications from dipolar contributions

do not arise. Whenever contributions from intramembrane interactions are appreciable, determination of the depth at which the spin label is located in the membrane requires an experimental calibration of the relaxation enhancement profile by using different positional isomers of spin-labeled lipids (e.g., the *n*-PCSLs). This method has been used previously with an electroneutral Ni^{2+} complex by Hubbell and co-workers [e.g. (*5*)]. Given that an empirical calibration must be performed, Cu^{2+} salts (or electroneutral complexes) are likely to provide stronger relaxation enhancements than those of Ni^{2+} because of potentially higher solubilities and additional contributions from intramembrane dipolar interactions.

Mn^{2+} ions provide additional distance-dependent enhancements by static dipolar interactions with the population of ions in the aqueous phase because of the higher spin of Mn^{2+}. These contributions may, however, be offset by a less favorable membrane solubility relative to Ni^{2+} ions. In addition, there is the technical complication of the background EPR signal in the $g = 2$ region from aqueous Mn^{2+} at ambient temperatures. Nevertheless, Mn^{2+} ions do provide a possibility for modulating the depth profile of enhancement by means of the characteristic depth-dependence of the dipolar contribution from ions in the aqueous phase. If one wishes to emphasize dipolar interactions from ions localized in the aqueous phase, at the expense of Heisenberg exchange, then Mn^{2+} is the most appropriate paramagnetic ion and sulfate should be chosen as the anion (to minimize penetration). To confine relaxation enhancements to contributions from ions in the aqueous phase, measurements should be made at low temperature in the lipid gel phase [cf. (*3*)].

Finally, the possibility of studying translational diffusion of paramagnetic ions in the membrane opens up the possibility of a new range of experiments that, being localized to different membrane regions, are complementary to oxygen transport studies (*48*, *49*) and therefore deserve further consideration. For this, Ni^{2+} ions and particularly the perchlorate salt seem especially suitable.

ACKNOWLEDGMENTS

We thank Frau B. Angerstein for synthesis of spin-labeled phospholipids. We are extremely grateful to Dr. K. Simon of the Geochemical Institute, University of Göttingen, for the atomic absorption measurements. This work was supported in part by the Deutsche Forschungsgemeinschaft. The work of V.A.L. and B.G.D. was also supported in part by RFBR Grant 98-03-33270.

REFERENCES

1. G. I. Likhtenstein, A. V. Kulikov, A. I. Kotelnikov, and L. A. Levchenko, Methods of physical labels—A combined approach to the study of microstructure and dynamics in biological systems, *J. Biochem. Biophys. Methods* **12,** 1–28 (1986).
2. C. Altenbach, T. Marti, H. G. Khorana, and W. L. Hubbell, Transmembrane protein structure: Spin labelling of bacteriorhodopsin mutants, *Science* **248,** 1088–1092 (1990).
3. T. Páli, R. Bartucci, L. I. Horváth, and D. Marsh, Distance measurements using paramagnetic ion-induced relaxation in the saturation transfer electron spin resonance of spin-labeled biomolecules. Application to phospholipid bilayers and interdigitated gel phases, *Biophys. J.* **61,** 1595–1602 (1992).
4. W. L. Hubbell and C. Altenbach, Site-directed spin labeling of membrane proteins, *in* "Membrane Protein Structure: Experimental Approaches" (S. H. White, Ed.), pp. 224–248, Oxford Univ. Press, New York, 1994.
5. C. Altenbach, D. A. Greenhalgh, H. G. Khorana, and W. L. Hubbell, A collision gradient method to determine the immersion depth of nitroxides in lipid bilayers: Application to spin-labeled mutants of bacteriorhodopsin, *Proc. Natl. Acad. Sci. USA* **91,** 1667–1671 (1994).
6. J. Voss, L. Salwinski, H. R. Kaback, and W. L. Hubbell, A method for distance determination in proteins using a designed metal ion binding site and site-directed spin labeling: Evaluation with T4 lysozyme, *Proc. Natl. Acad. Sci. USA* **92,** 12295–12299 (1995).
7. S. Paula and D. W. Deamer, Membrane permeability barriers to ionic and polar solutes, *in* "Current Topics in Membranes," Vol. 48 (D. W. Deamer, A. Kleinzeller, and D. M. Fambrough, Eds.), pp. 77–95, Academic Press, San Diego, 1999.
8. A. Finkelstein, Water and nonelectrolyte permeability of lipid bilayer membranes, *J. Gen. Physiol.* **68,** 127–135 (1976).
9. M. K. Jain, "The Bimolecular Lipid Membrane," 470 pp., Van Nostrand, New York, 1972.
10. Y. Cheng, X. Han, P. Schlesinger, and R. W. Gross, Nonesterified fatty acids induce transmembrane monovalent cation flux: Host–guest interactions as determinants of fatty acid-induced ion transport, *Biochemistry* **37,** 9497–9508 (1998).
11. J. Brunner, D. E. Graham, H. Hauser, and G. Semenza, Ion and sugar permeabilities in lecithin bilayers: Comparison of curved and planar bilayers, *J. Membr. Biol.* **57,** 133–141 (1980).
12. G. Cevc and D. Marsh, "Phospholipid Bilayers. Physical Principles and Models," Wiley–Interscience, New York, 1987.
13. J. Gutknecht, Cadmium and thallous ion permeabilities through lipid bilayer membranes, *Biochim. Biophys. Acta* **735,** 185–188 (1983).
14. D. Marsh, Progressive saturation and saturation transfer ESR for measuring exchange processes of spin-labelled lipids and proteins in membranes, *Chem. Soc. Rev.* **22,** 329–335 (1993).
15. D. Marsh, T. Páli, and L. I. Horváth, Progressive saturation and saturation transfer EPR for measuring exchange processes and proximity relations in membranes, *in* "Biological Magnetic Resonance, Vol. 14, Spin Labeling. The Next Millenium" (L. J. Berliner, Ed.), pp. 23–82, Plenum Press, New York, 1998.
16. T. Páli, L. I. Horváth, and D. Marsh, Continuous-wave saturation of two-component, inhomogeneously broadened, anisotropic EPR spectra, *J. Magn. Reson. A* **101,** 215–219 (1993).
17. V. A. Livshits, T. Páli, and D. Marsh, Relaxation time determinations by progressive saturation EPR: Effects of molecular motion and Zeeman modulation for spin labels, *J. Magn. Reson.* **133,** 79–91 (1998).
18. D. Marsh and A. Watts, Spin-labeling and lipid–protein interactions in membranes, *in* "Lipid–Protein Interactions, Vol. 2" (P. C. Jost and O. H. Griffith, Eds.), pp. 53–126, Wiley–Interscience, New York, 1982.
19. P. Fajer and D. Marsh, Microwave and modulation field inhomogeneities and the effect of cavity Q in saturation transfer ESR spectra. Dependence on sample size, *J. Magn. Reson.* **49,** 212–224 (1982).
20. A. V. Kulikov and G. I. Likhtenstein, The use of spin relaxation

phenomena in the investigation of the structure of model and biological systems, *Adv. Mol. Relax. Proc.* **10,** 47–79 (1976).

21. J. S. Hyde, H. M. Swartz, and W. E. Antholine, The spin–probe–spin label method, *in* "Spin Labelling II. Theory and Applications" (L. J. Berliner, Ed.), pp. 71–113, Academic Press, New York, 1979.
22. H. L. Friedman, M. Holz, and H. G. Hertz, EPR relaxation of aqueous Ni^{2+} ion, *J. Chem. Phys.* **70,** 3369–3383 (1979).
23. U. Lindner, Protonenrelaxation in paramagnetischen Lösungen unter Berücksichtigung der Nullfeldaufspaltung, *Ann. Physik* (*Leipzig*) **B16,** 319–335 (1965).
24. D. Fiat, Z. Luz, and B. L. Silver, Solvation of Co(II) in methanol and water enriched in oxygen-17, *J. Chem. Phys.* **49,** 1376–1379 (1968).
25. L. Banci, I. Bertini, and C. Luchinat, "Nuclear and electron relaxation. The magnetic nucleus-unpaired electron coupling in solution," VCH, Weinheim, 1991.
26. J. Reuben and D. Fiat, Nuclear magnetic resonance studies of solutions of rare-earth ions and their complexes. IV. Concentration and temperature dependence of the oxygen-17 transverse relaxation in aqueous solutions, *J. Chem. Phys.* **51,** 4918–4927 (1969).
27. L. Banchi, I. Bertini, F. Brigandi, and C. Luchinat, The electron-nuclear dipolar coupling in slow rotating systems. 4. The effect of zero-field splitting and hyperfine coupling when $S = 5/2$ and $I = 5/2$, *J. Magn. Reson.* **66,** 58–65 (1986).
28. A. McLaughlin, G. Gratwohl, and S. Mclaughlin, The adsorption of divalent cations to phosphatidylcholine bilayer membranes, *Biochim. Biophys. Acta* **513,** 338–357 (1978).
29. A. Abragam and B. Bleaney, "Electron Paramagnetic Resonance of Transition Ions," Clarendon Press, Oxford, 1970.
30. J. S. Leigh, Jr., ESR rigid-lattice line shape in a system of two interacting spins, *J. Chem. Phys.* **52,** 2608–2612 (1970).
31. Yu. N. Molin, K. M. Salikhov, and K. I. Zamaraev, "Spin Exchange. Principles and Applications in Chemistry and Biology," Springer Series in Chem. Physics 8 (J. P. Toennies and V. I. Goldanski, Eds.), Springer-Verlag, Heidelberg, 1980.
32. A. Abragam, "The Principles of Nuclear Magnetism" (W. C. Marshall and D. H. Wilkinson, Eds.), pp. 289–305. Oxford Univ. Press, Oxford, 1961.
33. B. Berner and D. Kivelson, Spin resonance line width method for measuring diffusion. A critique, *J. Phys. Chem.* **83,** 1406–1412 (1979).
34. A. Seidell, "Solubilities of Inorganic and Metal Organic Compounds," 3rd ed., Vol. I, Van Nostrand, New York, 1940.
35. "Gmelins Handbuch der Anorganischen Chemie," Verlag Chemie GmbH, Achte Auflage, 1938–1995.
36. B. L. Bales, Inhomogeneously broadened spin-label spectra, *in* "Biological Magnetic Resonance," Vol. 8 (L. J. Berliner and J. Reuben, Eds.), pp. 77–130, Plenum, New York, 1989.
37. I. Bertini and C. Luchinat, "NMR of Paramagnetic Molecules in Biological Systems," 319 pp., Benjamin/Cummings, Menlo Park, CA, 1986.
38. "CRC Handbook of Physics and Chemistry," 77th ed. (D. R. Hide, Ed.), CRC Press, Boca Raton, FL, 1996/1997.
39. W. K. Subczynski, A. Wisniewska, and J. J. Yin, Hydrophobic barriers of lipid bilayer membranes formed by reduction of water penetration by alkyl chain unsaturation and cholesterol, *Biochemistry* **33,** 7670 (1994).
40. D. Marsh, "Handbook of Lipid Bilayers," 387 pp., CRC Press, Boca Raton, FL, 1990.
41. L. Dalton, J. O. McIntyre, and S. Fleischer, Distance estimate of the active center of D-β-hydroxybutyrate dehydrogenase from the membrane surface, *Biochemistry* **26,** 2117–2130 (1987).
42. D. A. Windrem and W. Z. Plachy, The diffusion-solubility of oxygen in lipid bilayers, *Biochim. Biophys. Acta* **600,** 655–665 (1980).
43. W. K. Subczynski and J. S. Hyde, The diffusion-concentration product of oxygen in lipid bilayers using the spin label T_1 method, *Biochim. Biophys. Acta* **643,** 283–291 (1981).
44. A. Walter and J. Gutknecht, Permeability of small nonelectrolytes through lipid bilayer membranes, *J. Membr. Biol.* **90,** 207–217 (1986).
45. P. Schatzberg, Diffusion of water through hydrocarbon liquids, *J. Polym. Sci. Part C* **10,** 87–92 (1968).
46. W. R. Lieb and W. D. Stein, Biological membranes behave as non-porous polymeric sheets with respect to the diffusion of non-electrolytes, *Nature* (*London*) **224,** 240–243 (1969).
47. K. Kinosita, Jr., and A. Ikegami, Reevaluation of the wobbling dynamics of diphenylhexatriene in phosphatidylcholine and cholesterol/phosphatidylcholine membranes, *Biochim. Biophys. Acta* **769,** 523–527 (1984).
48. W. K. Subczynski, J. S. Hyde, and A. Kusumi, Oxygen permeability of phosphatidylcholine-cholesterol membranes, *Proc. Natl. Acad. Sci. USA* **86,** 4474–4478 (1989).
49. W. K. Subczynski, J. S. Hyde, and A. Kusumi, Effect of alkyl chain unsaturation and cholesterol intercalation on oxygen transport in membranes: A pulse ESR spin labeling study, *Biochemistry* **30,** 8578–8590 (1991).
50. H. Träuble, The movement of molecules across lipid membranes. A molecular theory, *J. Membr. Biol.* **4,** 193–208 (1971).
51. R. J. Pace and S. I. Chan, Molecular motions in lipid bilayers. III. Lateral and transverse diffusion in bilayers, *J. Chem. Phys.* **76,** 4241–4247 (1981).
52. D. Marsh and A. Watts, ESR spin label studies, *in* "Liposomes: From Physical Structure to Therapeutic Applications" (C. G. Knight, Ed.), Ch. 6, pp. 139–188, Elsevier/North-Holland Biomedical Press, Amsterdam, 1981.
53. M. B. Schneider, W. K. Chan, and W. W. Webb, Fast diffusion along defects and corrugations in phospholipid $P_{\beta'}$, liquid crystals, *Biophys. J.* **43,** 157–165 (1983).